IDENTIFICATION OF CIRCULAR RIBONUCLEIC ACIDS DIFFERENTIALLY EXPRESSED IN APOPTOTIC HeLa CELLS

A Thesis Submitted to
the Graduate School of Engineering and Sciences of
İzmir Institute of Technology
in Partial Fulfillment of the Requirements for the Degree of

MASTER OF SCIENCE

in Molecular Biology and Genetics

by
Bilge YAYLAK

July 2018
İZMİR

We approve the thesis of **Bilge YAYLAK**

Examining Committee Members:

Assoc. Prof. Bünyamin AKGÜL,
Department of Molecular Biology and Genetics, Izmir Institute of Technology

Prof. Volkan SEYRANTEPE,
Department of Molecular Biology and Genetics, Izmir Institute of Technology

Assoc. Prof. Duygu SAĞ,
Izmir Biomedicine and Genome Center, Dokuz Eylul University

9 July 2018

Assoc. Prof. Bünyamin AKGÜL
Supervisor, Department of Molecular Biology and Genetics,
İzmir Institute of Technology

Prof. Volkan SEYRANTEPE
Head of Department of Molecular
Biology and Genetics

Prof. Aysun SOFUOĞLU
Dean of Graduate School of
Engineering and Sciences

ACKNOWLEDGEMENTS

First of all, I would like to express my very great appreciation to my supervisor Assoc. Prof. Bünyamin AKGÜL for his valuable and constructive suggestions, patience, understanding and encouragement during my graduate studies. I want to indicate my regards and thanks to TUBITAK (Scientific and Technological Research Council of Turkey) due to their support and fund (Project No: 215Z081).

I would like to thank the committe member, Prof. Volkan SEYRANTEPE for their support and sharing his laboratory and materials during my study. Furthermore, kind thanks to Prof. Yusuf BARAN to let me use his laboratory materials and to committe member Assoc. Prof. Duygu SAĞ due to her time for supporting my thesis.

Special thanks should be given to Dr. İpek ERDOĞAN, our post-doc, for her valuable technical support, her moral, friendship, patience and guidance throughout my study. Likewise, much thanks to my other colleagues, Bengisu GELMEZ for her friendship and guidance, Osama SWEEF, M. Caner YARIMÇAM, Dilek Cansu GÜRER and Ayşe Hale GÜÇKIR for their extra interest and help in dealing with experiments. I am also thankful to Biotechnology and Bioengineering Central Research specialist Dane RUSÇUKLU for her kind help during studies.

I wish to declare my deepest thanks to my family for their love, my beloved persons in my life – to Bahar LAFÇİ and Esra AYDIN for their support, motivation and faith during my graduate life.

ABSTRACT

IDENTIFICATION OF CIRCULAR RIBONUCLEIC ACIDS DIFFERENTIALLY EXPRESSED IN APOPTOTIC HELA CELLS

Apoptosis is a mechanism of programmed cell death that is essential for survival, homeostatis and development. Various protein coding genes and non-coding RNAs were reported as apoptosis regulators. However, the potential roles of circular RNA in the regulation of apoptosis are still unknown. In this study, we have performed transcriptomics study to reveal differentially expressed, pathway-drug specific and/or global circRNAs in apoptotic HeLa cells. Cisplatin (CP), doxorubicin (DOX), Fas mAb(FAS) and TNF-alpha (TNF-a) were used to trigger apoptosis in HeLa cells. Apoptosis rates of three replicates of treatment and control cells were measured by flow cytometry and differentially expressed circular RNAs were identified by deep RNA sequencing. Circular RNA candidates were firstly sorted based on their significance according to pad j value, further classified based on fold change, pathway-drug specificity and source genes. Then, circular RNA candidates were analysed bioinformatically to obtain their coding potential, potential miRNA binding sites and involvement in possible apoptotic pathways. Furthermore, divergent primers were designed to validate backsplicing junction sequence of circular RNA candidates. RNAse R treatment was used to eliminate linear transcripts and enrich circular RNAs. The expression of candidate circular RNAs was analysed RNAse R treated samples. Backsplicing junctions of positive circular control circ-HIPK3 was validated by TA cloning and sequencing. Differential expression of positive control (circ-HIPK3), candidate-8 and candidate-6 were validated by quantitative PCR.

Key words: apoptosis, circular RNAs, deep sequencing, RNase R, transcriptomics

ÖZET

APOPTOTİK HELA HÜCRELERİNDE FARKLI İFADE EDİLEN HALKASAL RİBONÜKLEİK ASİTLERİN TANIMLANMASI

Apoptoz, hayatta kalma, dengeleşim ve gelişim için gerekli olan programlanmış hücre ölümü mekanizmasıdır. Çeşitli protein kodlayan genler ve kodlayıcı olmayan RNA'lar apoptoz regülatörleri olarak rapor edilmiştir. Bununla birlikte, apoptozis regülasyonunda halkasal RNA'nın potansiyel rolleri hala bilinmemektedir. Bu çalışmada, apoptotik HeLa hücrelerinde farklı şekilde ifade edilen, yolak-ilaç spesifik ve / veya global halkasal RNA'ları ortaya çıkarmak için transkriptomik çalışma gerçekleştirdik. HeLa hücrelerinde apoptozu tetiklemek için sisplatin, doksorubisin, Fas mAb ve TNF-alfa kullanılmıştır. İlaçla muamele edilmiş hücreler ve kontrol hücrelerinin üç tekrarının apoptoz oranı akış sitometrisi ile ölçülmüş, farklı şekilde ifade edilen halkasal RNA'lar derin RNA dizilemesi ile tanımlanmıştır. Farklı olarak ifade edilen halkasal RNA adayları, ilk olarak padj değeri baz alınarak anlamlılıklarına göre sıralanmış daha sonra kat değişimi, yolak-ilaç spesifisitesine ve kaynak aldıkları genlere dayalı olarak sınıflandırılmıştır. Daha sonra, halkasal RNA adayları, onların kodlama potansiyellerini, potansiyel mikro RNA bağlama bölgelerini ve olası apoptotik yolaklara katılımlarını elde etmek için biyoinformatik olarak analiz edilmiştir. Ayrıca ıraksak primerler halkasal RNA adaylarının geri birleşme bağlantı dizisini doğrulamak için tasarlanmıştır. Lineer transkriptleri ortadan kaldırmak ve halkasal RNA'ları zenginleştirmek için RNAse R uygulaması yapılmıştır. Halkasal RNA adaylarının ifadesi RNAse R ile muamele edilmiş örnekte analiz edilmiştir. Halkasal pozitif kontrolün geri birleşme bağlantı dizisi TA klonlama ve dizileme ile doğrulanmıştır. Pozitif kontrol (circ-HIPK3), aday-8 ve aday-6 nın farklı ifadesi kantitatif PCR ile doğrulanmıştır.

Anahtar kelimeler: apoptoz, halkasal RNA, derin dizileme, RNase R, transkriptomiks.

TABLE OF CONTENTS

LIST OF FIGURES

LIST OF TABLES

CHAPTER 1

INTRODUCTION

1.1. Apoptosis

PCD (Programmed Cell Death) mediates the balance between survival and cell death. Abnormal regulation of PCD is associated with a variety of diseases, comprising developmental and immunological disorders (Fuchs et al., 2011). Apoptosis, autophagy and programmed necrosis are three main forms of PCD, which are easily distinguished due to their key morphological differences (Tan et al., 2009; Bialik et al., 2010).

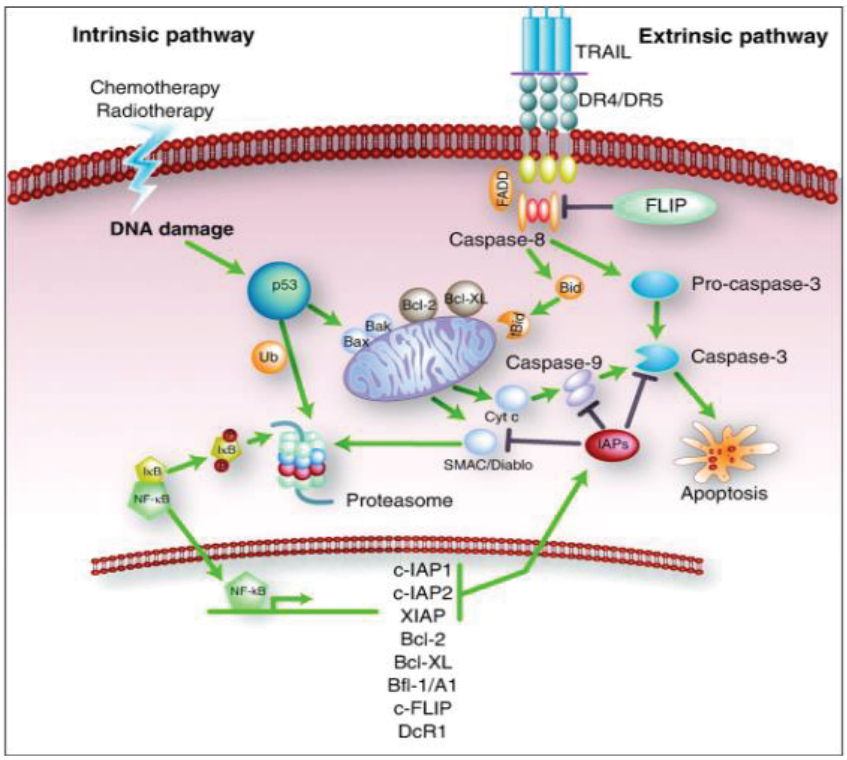

Figure 1.1. Schematic representation of apoptotic pathways. Apoptosis divides into two main pathway as intrinsic and extrinsic. In general death receptors such as FAS and TRAIL, which can activate caspase-8 and caspase-3, are involved in extrinsic pathway. Intrinsic pathway is triggered by stress signal and DNA damage via mitochondria. Caspase-dependent and -independent pathways are subgroups of mitochondria mediated intrinsic apoptosis pathway. (Source: de Vries et al., 2006)

Apoptosis is a mechanism of type 1 programmed cell death and it is vital for homeostatis and development. It was described by Kerr et al. (1972) firstly. Cell stress stimulates pro apoptotic signalling pathways which activate caspase proteases and results in mitochocondrial dysfunction.

Apoptotic cells undergo characteristic changes in cell morphology including cell shrinkage, chromatin condensation, cell rounding, plasma membrane blebbing, nuclear fragmentation and budding respectively (Kerr et al., 1972). After that, cell fragments seperate into apoptotic bodies that consist of cytoplasm with packaged organelles that can be with or without nuclear fragments. Macrophages, parenchymal or neoplastic cells take up these bodies with phagocytic activity that then degregade within phagolysosomes (Kurosaka et al., 2003, Vitale et al., 2018).

The understanding of the mechanistic machinery of apoptosis at the molecular level is important because PCD is a component of both disease and health. Therefore, this widespread involvement of apoptosis in the pathophysiology of disease contributes to therapeutic intervention at many different checkpoints. Moreover, understanding the mechanism of apoptosis provides deeper insight into various disease processes (Bright et al., 1994).

1.2. Mechanism of Apoptosis

1.2.1. Caspase Dependent Mechanism

Apoptosis is a morphological phenomenon. Mechanism of apoptosis is highly sophisticated which involves an energy dependent cascade of molecular events. Up to date, two main pathways have been discovered which are extrinsic and intrinsic or mitochondrial pathway. However, research indicates that both of pathways are linked and so any molecules in one pathway can be influenced by the other (Igney and Krammer, 2002).

There is an additional way of cell death that involves T-cell mediated cytotoxicity and perforin-granzyme-dependent cell death. Apoptosis can be induced by perforin/granzyme pathway with either granzyme A or granzyme B. The granzyme B pathways, extrinsic and intrinsic pathways share the same execution pathway initiated by the cleavage of caspase-3 and results in formation of apoptotic bodies, cross-linking of

proteins, degredation of cytoskeletal and nuclear proteins and DNA fragmentation. The granzyme A pathway activates a parallel, caspase-independent cell death pathway via single stranded DNA damage (Martinvalet et al., 2005).

Caspases are extensively expressed in most cells in an inactive proteoenzyme form. Once they are activated, they can often activate other procaspases. This allows initiation of a protease cascade. This proleolytic cascade results in amplification of apoptotic signalling pathway and therefore leads to rapid cell death (Elmore et al., 2007).

1.2.1.1. Intrinsic Apoptosis Pathway

Intrinsic apoptosis is initiated by several microenvironmental perturbations such as growth factor withdrawal, DNA damage, endoplasmic reticulum (ER) stress, ROS overload, microtubular alterations, mitotic defects or replication stress. Plasma membrane integrity and metabolic activity of apoptotic cells are retained to some degree. All of these stimuli result in inner mitochondrial permeability transition (MPT) pore opening. It causes loss of the mitochondrial transmembrane potential, so two main groups of pro apoptotic proteins, which are normally sequestered are release from the intermembrane space into the cytosol (Saelens et al., 2004).

Cytochrome c, Smac/DIABLO and the serine protease HtrA2/Omi get involved in first group (Elmore, 2007). Cytochrome c activates the caspase dependent pathway by binding and activating Apaf-1 as well as procaspase-9 and forming an “apoptosome” (Chinnaiyan, 1999; Hill et al., 2004). On the other hand, Smac/DIABLO and the serine protease HtrA2/Om are reported to induce apoptosis by inhibiting inhibitors of apoptosis proteins (IAP) activity (Saelens et al., 2004).

The critical step for apoptosis is widespread and irreversible mitochondrial outermembrane permeabilization (MOMP) (Tait SW et al., 2010). This is regulated by anti-apoptotic and pro-apoptotic members of the BCL-2, apoptosis regulator BCL-2 protein family. These group of proteins share one of four BCL homology domains (BH1, BH2, BH3, BH4) (Pena-Blanco et al., 2017). MOMP is mediated by Bcl-2 associated X, BAX and/or BAK in response to apoptotic stimuli. BAX and BAK with BOK are the only BCL2 family members with an ability to create pores across the outer mitochondrial membrane (OMM) in mammalian cells (PE et al., 2014). BAX cycles between the cytosol and the OMM continously (Edlich et al., 2016).

The BCL-2 (B-cell lymphoma 2) family proteins are highly important in the control and regulation of intrinsic apoptotic pathway.

This family can be either pro- or anti- apoptotic and these proteins are regulated by p53, the tumor supressor protein. BCL-2, BCL-x, BCL-xl, BCL-xs, BCL-w and BAG are anti-apoptotic members of BCL-2 family proteins. Some of pro-apoptotic members are BCL-10, Bax, Bak, Bid, Bak and Blk (Taylor et al., 2008).

1.2.1.2. Extrinsic Apoptosis Pathway

In the receptor-mediated programmed cell death pathway, the death signal for the PCD is triggered by an external stimulus. The extrinsic apoptosis pathway is stimulated through activation of death receptors of the tumor necrosis factor (TNF) family, including the TNF receptor 1 (TNF-R1), CD95 (APO-1, Fas), TNF-related apoptosis-inducing ligand (TRAIL) receptors (TRAIL-R1 and TRAIL-R2), DR3 and DR6. The extrinsic pathway can crosstalk with the intrinsic pathway via cleavage of Bid.(Jin et al., 2005).

Signalling through both CD95 (APO-1, FAS) and TRAIL-R1/-R2 (TNF related apoptosis inducing ligand) lead to formation of death-inducing signalling complex (DISC). This complex simultaneously activates Caspase 8 and 10. Binding of antibodies or agonistic ligands leads to death receptor oligomerization followed by FADD (Fas-associated protein with death domain) or TRADD recruitment.

Pro-caspase 8 residues are recruited and bind to create a multi protein complex. FADD and pro-caspase-8 possess a homologous region called “death effector domain” (Hsu et al., 1995; Kelliher et al., 1998; Wajant, 2002). These interactions lead to cleavage of two pro-caspase-8 to produce an active caspase-8. Executioner caspases, which are caspase -3 -6 and -7 are activated by caspase-8 and carry out the self destruction process, which is characterized by morphoogical changes, of the cell (Ricci et al., 2007).

Another common extrinsic pathway of apoptosis is by the killer lymphocytes through Fas protein and Fas ligand. Fas ligand is produced by killer lymphocytes and triggers apoptosis by binding to its receptor on plasma membrane of the target cell. Fas protein can recruit intracellular adapter proteins which can aggregate with pro-caspase-8. Downstream pathways which is activated by caspase 3 are activated by caspase-8 (Griffith et al., 1995).

1.2.1.3. Execution Pathway

The final pathway of apoptosis is carried out by executioner or effector caspases. Execution pathway is the final step of both intrinsic and extrinsic pathway. Caspase-3, -6 and -7 are called activated execution caspases which are involved in activation of cytoplasmic endonuclease and proteases; cleavage of cytokeratins, PARP, alpha fodrin, the nuclear protein NuMa. To sum up, nuclear material degredation, morphological and biochemical changes in apoptotic cells are governed by execution caspases. Among execution caspases, caspase-3, which is activated by caspase-8, -9, -10, is most valuable one (Slee et al., 2001; Kothakota et al., 1997).

1.2.2. Caspase Independent Pathway

Pro-apoptotic proteins, which include apoptosis inducing factor (AIF), caspase activated DNase (CAD) and endonuclease G, are released from the mitochondria during apoptosis. This occurs after the cell has committed to die. DNA fragmentation and early form peripheral nuclear chromatin condensation (stage I) occur after transcolation of AIF to the nucleus (Josa et al., 2001). Endonuclease G also translocates to the nucleus and oligonucleosomal DNA fragments are produced where endonuclease G cleaves nuclear chromatin. Both AIF and endonuclease G function in caspase-independent manner (Susin et al., 2000; Li et al., 2001). CAD is released from the mitochondria and translocates to the nucleus where it results in oligonucleosomal DNA fragmentation and stage II chromation condensation after cleavage by caspase-3 (Enari et al., 1998).

1.3. Circular RNAs

Circular RNAs are single stranded and covalently closed transcripts comprising many RNA species. First investigation of circular RNAs which are produced from precursor mRNAs, was reported in more than 20 years ago (Greene et al., 2017). However, until 2000s circular RNAs were thought to be transcript artifacts. Widespread expression of circular RNAs was shown by development of RNA-seq of non-polyadenylated transcriptome technology. Although the overall functions of circular

RNAs are unknown, recent studies reveal that some circular RNAs have important roles in gene regulation. For example, circular RNAs can be produced by over 10% of expressed genes in cells and tissues (Jeck et al., 2014; Szabo et al., 2016).

Circular RNAs are newly discovered noncoding RNAs with 3' and 5' termini that represent start and stop site of the RNA polymerase on template DNA (Wang et al., 2017; Memczak et al., 2013). Covalent linkage of the end of the single RNA molecules to create circRNA is rare events unlike splicing reactions between different RNA molecules (trans-splicing) (Wang et al., 2017; Memczak et al., 2013). Circular RNAs had been regarded as accidental byproduct of post transcriptional errors due to their low levels of expression. Their important functions in multiple biological processes were identified with the development of bioinformatics and use of RNA deep sequencing technology (Qu et al., 2015). In that point, RNAse R treatement before deep sequencing is useful as circular RNAs are resistant to RNAse R treatment (Jeck et al., 2014).

CircRNAs are largely generated from exonic or intronic sequences and highly abundant in eukaryotic transcriptome (Zhang et al., 2013). Although they are generally expressed at low levels, recent discoveries have revealed new insight into their cell or tissue spesific expression. Additionally hundreds of undescribed intronic lncRNAs from the polyA(-) RNA- seq were identified as circular RNAs (Zhang et al., 2013).

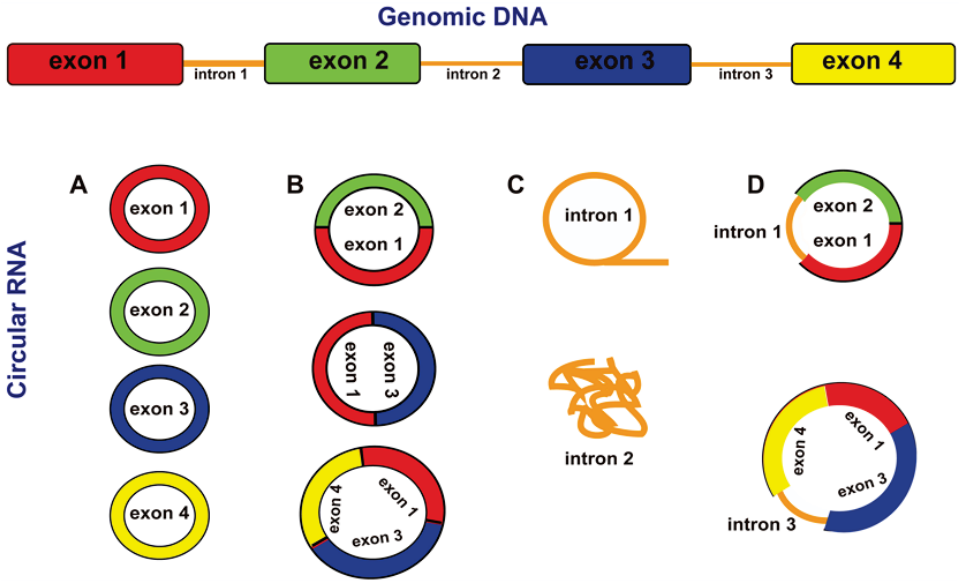

Figure 1.2. Figure shows a model for circular RNAs transcription from one gene by different circular RNAs. (Source: Andreeva and Cooper, 2015)

RNA sequencing fosters investigations of novel alterations and fluctuations in the sequence, expression and structure of transcriptomes (Jeck et al., 2014). Until recently circular RNAs have eluded detection as they were considered library preparation artifacts. Normally, miRNAs or other small RNAs rather than circular RNAs are easily separated from other RNA types based on their electrophoretic mobility or size. However, molecular techniques that involve either fragmentation or amplification destroy circularity and interfere with detection of circular RNAs. The absence of cap or a tail excludes RACE as an alternative approach (Jeck et al., 2014).

For circRNA biogenesis, RBPs (RNA binding proteins) and reverse complementary sequences (RCS) are necessary (Jeck et al., 2014). Highly abundant RCS between introns bracketing circRNAs were reported (Chen et al., 2015) by scoring RCS in human introns leading to circular RNA prediction and validation.

First covalently closed circular RNA molecules were reported in plants as uncoated infectious RNA molecules called viroids in 1976 (Sanger et al., 1976). First animal virus identified with a circular RNA genome is Hepatitis delta $\wp$ virus that was reported in 1986 (Kos et al., 1986). As known, splice site juxtaposition is required for correct ligation of exons from pre-mRNA, generally involving in a downstream 3' and upstream 5' splicesite. In 1991, it was reported that splicing of upstream 3' and downstream 5' splicesite result in circular RNA formation. This mode of splicing was speculated to represent rare RNAs containing scrambled exons (Nigro et al., 1991). Later, endogenous circular RNAs stemming from pre- mRNA were identified in mouse Sry (Capel et al., 1993). After that, in 1996, circRNAs were reported to consist of exons from RNA transcripts in human cells (Pasman et al., 1996). Up to now, the number of reported circular RNAs has risen in parallel to advances in sequencing technology.

1.3.1. Biogenesis of Circular RNAs

Biogenesis of circular RNAs can be divided into three pathways;

Spliceosome-dependent biogenesis**.** Canonical spliceosomeal machinery is required for the processing of the back-splicing reaction. Thus, exon circularization efficiency is directly dependent on the presence of canonical splice sites which bracket the exons. However, in general, canonical splicing efficiency seems to be much higher than that of back-splicing. Thus, the steady-state levels of circular RNAs are much lower

than those of their linear counterparts. Mechanistic machinery of splicesome involvement in back splicing is unclear. However, ongoing studies using *in vitro* back-splicing assays carried out in nuclear extracts might give additional information about mechanistic insight into circular RNA biogenesis. Circularization may occur both post- and co-transcriptionally (Chen et al., 2016).

Cis-Elements provide circular RNA formation. Most circular RNAs have several exons generally two or three. Therefore, it can be said that there are no spesific exon sequences avaliable to facilitate circularization. Moreover, alternative splicing can produce lots of circular RNAs, with or without internal intron, from the same gene. However, it is reported that back-splicing may require a minimal exon length. Regulatory elements residing in the flanking introns of the circularized exon are required for back-splicing. The majority of circular RNAs, which are processed from long flanking introns and internal exons, generally contains reverse complementary sequences. These reverse complementary sequences have pairing ability to form RNA duplexes that enhance backsplicing (Chen et al., 2016).

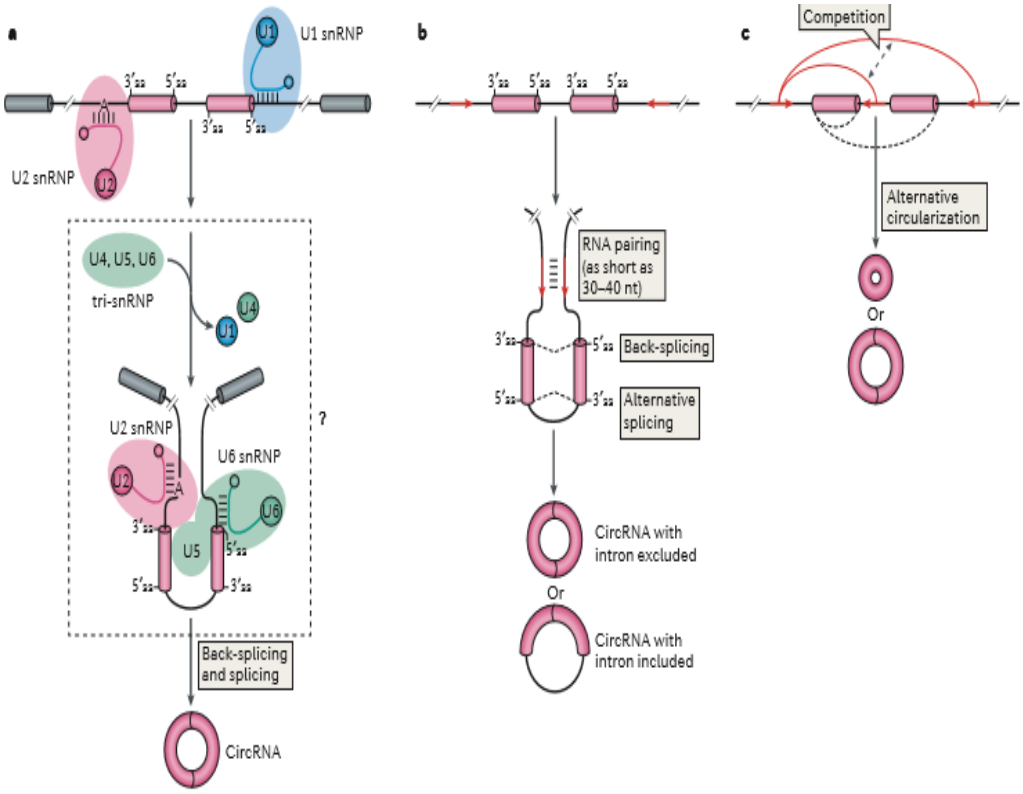

Figure 1.3. Schematic representation of circular RNA biogenesis and its regulation. Circular RNAs are produced by backsplicing reaction via spliceosomal machinery. (Source: Chen et al., 2016)

RNA pairing can take place either from non-repetetive complementary sequences or at repetetive elements. Thirty-to-fourty nt long sequences are enough to perform circular RNA biogenesis. Competition of RNA pairing between flanking introns and within individual introns directly affects back-splicing efficiency as well. In addition, reverse oriented *Alu* elements in introns can form variable *Alu* pairs, theoretically and promote production of different circular RNAs which are originated from a single gene (Chen et al., 2016).

Not all circular RNAs have flanking complementary sequences. This observation suggest that any *cis* elements in the intronic sequences have important effect on circular RNA production. However, RNA binding proteins can recognize short *cis*-regulatory elements in introns and promote exon circularization (Chen et al., 2016).

Regulation of circular RNA formation by RNA binding proteins. KH Domain RNA Binding Protein (QKI) is an important example that regulates circular RNA production from its own pre-mRNA. During epithelial-to- mesenchymal transition, many circular RNAs are upregulated by QKI. This suggests that circular RNAs can be purposefully produced in a tissue or cell type spesific manner. Mechanistic machinery of QKI dependent circular RNA formation basically depends on binding of QKI to the circularized exon and close them together. Adenosine-to-inosine editing is carried on by ADAR1, which diminishes the annealing of duplexed RNAs formed among sequences flanking circularized exon followed by backsplicing reduction (Chen et al., 2016).

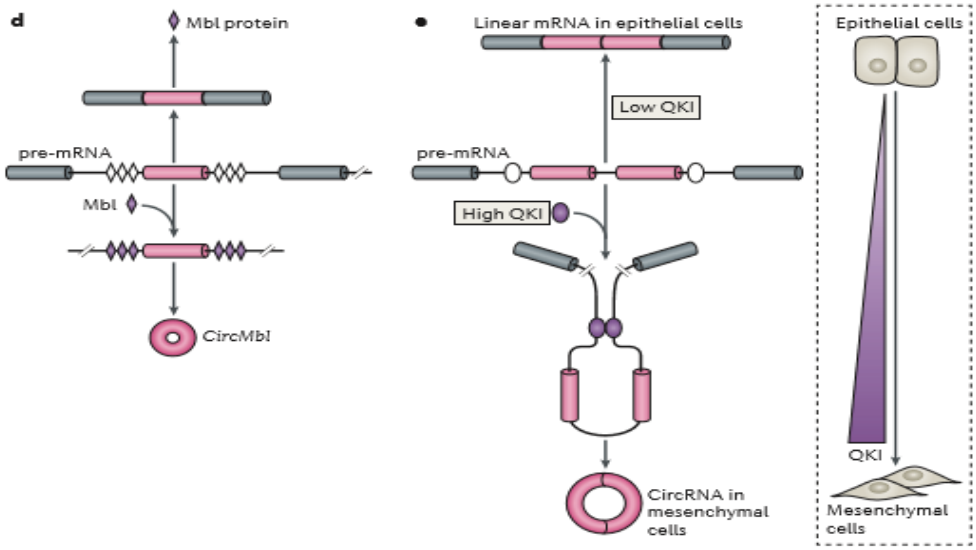

Figure 1.4. Binding of mannose-binding lectin (Mbl) protein to introns bracketing the circularized exon promotes circular RNA biogenesis from its own gene. (Source: Chen et al., 2016)

1.3.2. Circular RNAs: Act of Mechanism in Gene Regulation

Circular RNA role in gene regulation depends on their exon-intron content, and localization as well as their miRNA and RBP binding sites. Gene regulation is affected by competative binding of circular RNA to spesific sites by changing the expression level either in positive or negative manner (Huang et al., 2017).

Circular RNAs act as miRNA sponges. Exonic circular RNAs interfere with miRNAs through the specific binding sites and block binding of miRNA to its target coding gene which results in miRNA-mediated posttranscriptional regulation. This phenomenon, which termed as sponging was firstly reported to explain a linear transcript with concatenated miRNA target sites artificially expressed in cells to reduce an endogenous miRNA. The best characterized circular RNA that uses explain miRNA sponging model is ciRS-7 produced from the CDR1 antisense transcript. CiRS-7 is highly expressed in both mouse and human brain and capable of binding up to 20,000 miR-7 molecules per cell. Sex-determining region Y (Sry) is function as a miRNA sponge as well, it has 16 target sites for miR-138 in mouse. It should be noted that miRNA target sites in circular RNAs do not need be conserved for sponging miRNA. Thus, some circular RNAs might not function as miRNA sponges (Huang et al., 2017).

Circular RNAs directly interacts with RNA polymerase II and U1 snRNP to regulate transcription. Major part of the circular RNAs located in the cytoplasm. However, intron containing circular RNAs (ElciRNA) were shown to be localized in the nucleus. Another class of circular RNAs called circular intronic RNA (ciRNA) are originated from lariat introns. In human, a variety of ciRNAs regulate gene expression in *cis*. Some well characterized ciRNAs such as ci-sirt7 and ci-ankrd52 accumulate in the nucleus and interact with the elongated RNA Polymerase II complex. Decrease in the amount of these circular RNA in cells reduces the transcription level of their parental genes ANKRD52 or SIRT7. Therefore, it can be suggested that ciRNAs promote pol II transcription of parental genes. Mechanism of action is unknown (Huang et al., 2017; Chen et al., 2016).

Exon-intron circular RNAs (ElciRNAs) are associated with Pol II. Depletion of circular RNAs such as ElciEIF3J and ElciPAIP2 decreased the transcription of their parental genes. Mechanistically, ElciRNA is associated with U1 snRNP and with their encoding gene promoters. Blocking the formation of ElciRNAs- U1 snRNP complex

results in a reduction in interaction betwen ElciRNA and PolII. Moreover, ElciRNAs- U1 snRNP complex can not interact with promoters of their encoding genes which reduce the transcription of these genes (Huang et al., 2017; Chen et al., 2016).

Alternative splicing. Circular RNAs are produced co-transcriptionally and single gene locus can be the source of different types of circular RNA by competitive complementarity of intron sequences. Thus, the canonical pre-mRNA splicing and circularization compete with each other. Moreover, alternative splicing occurs because of disappearance of internal exons after backsplicing. It was reported that exon skipping which is the most famous alternative splicing event in pre-mRNA, was positively correlated with circular RNA production. Thus, circular RNA formation might modulate gene expression by decreasing linear mRNA level. Additionally, it should be noted that if circularized exon contains translation start site, translation of remaining truncated linear mRNA will be fail. Thus, protein level of linear mRNA can be affected as well (Huang et al., 2017; Chen et al., 2016).

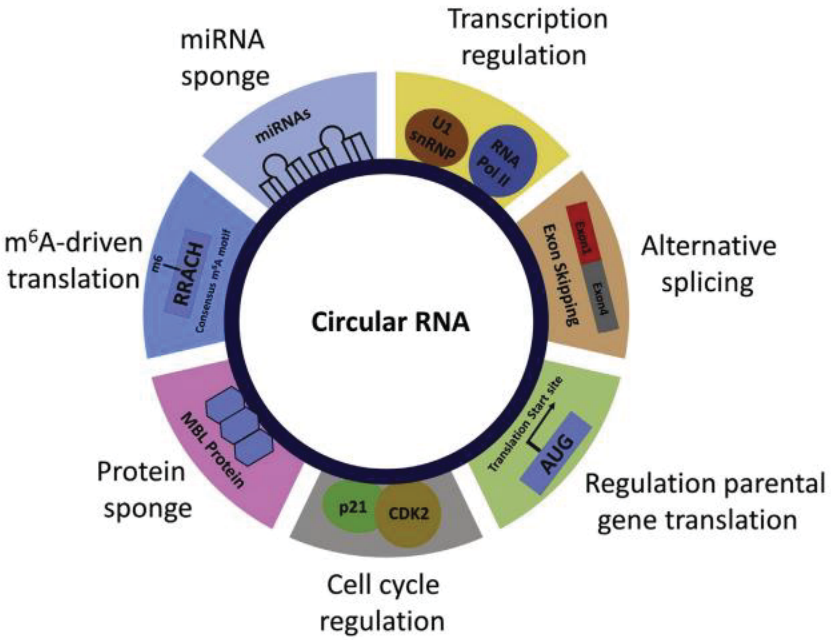

Figure 1.5. Schematic representation of gene regulation by circular RNA. (Source: Huang et al., 2017)

Protein binding. Interaction with RNA binding proteins also regulate transcription. Circular RNA circ-foxo3, that is primarily expressed in non-cancerous

cells, can block the function of CDK2 via producing circ-foxo3-p21-CDK2 ternary complex. CircMbl, derived from MBNL1 in humans, is another common example of protein binding circRNA, which binds to Mbl protein directly. Meanwhile Mbl protein can associate with flanking introns to facilitate exon circularization. Therefore, Mbl parental gene might regulate its own protein level through promoting circMbl production and then sponging excess Mbl protein (Huang et al., 2017; Chen et al., 2016).

Translation. The majority of the circular RNAs are derived from exons and localized in the cytoplasm; thus, an interesting question is whether circular RNAs could be translated. Interestingly, circular RNAs contain consensus N^6 methyladenosine (m^6A) motifs and one of these motifs is sufficient to initiate translation. Eukaryotic ribosomes can initiate translation by only the target RNA contains IRES element (Huang et al., 2017; Chen et al., 2016; Yang et al.,2017).

1.3.3. Experimental and Computational Approaches for Circular RNA Identification

Currently existing circular RNA identification methods are generally based on detection of backsplicing junction (BSJ) reads. “Backsplice” is an out-of-order arrangement of exons and a key feature of circular RNA (Jeck et al., 2014). It should be noted that it is not exclusive to circRNA. Thus, such sequences were filtered out by previous version of RNA-seq mapping algorithms. Notably, some different mechanisms other than formation of circular RNA such as reverse transcriptase template switching, RNA transsplicing and tandem duplication can cause production of these apparent backsplice sequences. These problems have newly been addressed through the development of novel bioinformatic tools, higher throughput and longer reads sequencing, sequencing of r-RNA depleted RNA libraries (Jeck et al., 2014). An ‘apparent backsplice’ sequence is defined as any case in which the ordering of the exons in a sequence is reversed relative to the annotated template. Additionally, several approaches are needed to distinguish such species from exonic circular RNA. Linear isoform of exonic RNAs have 3’ polyadenylation, however circles have not. Furthermore, linear RNAs migrate much faster in a gel than exonic circular RNA of the same length. Exonic circular RNA has less nucleotide sequence than full, tandem duplicated or trans-spliced circRNAs. In order to assess these characteristics, standard northern blot can be

used. Moreover, RNAse H degradation observation is a more conclusive way to prove existance of circular RNA, because circular RNA can be turned into single linear product of a predictable size after RNAse H degradation. RNAse R exonuclease do not harm circular RNA and leave them intact but adequately degrade most linear RNAs (Jeck et al., 2014).

Non-uniformity of RNA-seq data sets and complicated nature of eukaryotic transcription may lead to false positive results. Also, parts of the most circular RNAs exist in low abundance compared with linear counterparts. Therefore, total RNAs used in RNA seq is generally enriched for circRNAs by eliminating linear RNA by RNAse R treatment (Gao et al., 2015).

Computational detection methods have been extensively used in circular RNA identification using either annotation-dependent (MapSplice, CIRCExplorer (most cited one), KNIFE) o,r *de novo* (find_circ, segemehl, CIRI, acfs, circRNA_finder) algorithms (Gao et al., 2017). However, these computational pipelines sometimes give false positive predictions based on RNase R resistance. Thus, in order to achieve reliable prediction, several tools should ideally be merged (Hansen et al., 2016). These methods have been developed to investigate nonlinear reads and finally anticipate the landscape of circular RNAs based on RNA seq datasets. Many circular RNAs are being identified and integrated into databases. Over 150,000 circRNAs, mature RNA sequences and genomes of various species are saved in the deepbase 2,0 and cirbase. Cir2Traits is a program designed to reach circRNAs and related diseases. CircRNAbase and CircNet contain not only alternatively spliced variants of circRNAs and their differential expressions in various cell lines and tissues but also possible miRNA regulated networks (Wang et al., 2017).

1.3.4. Circular RNA Regulatory Role in Apoptosis

To date, RNA seq and newly developed bioinformatic methods allowed the identification of several circular RNAs involved in mechanisms determining cell fate such as apoptosis. Efforts to understand of circular RNA involvement in apoptosis include studies performed on diseases such as cardiac hyperthrophy, neurodegenerative diseases and atherosclerosis models (Mehta et al., 2017; Dang et al., 2017; Wang et al., 2017; Nan et al., 2016).

Mehta et al. identified 13 circular RNAs in brain stroke in adult mice after induction of focal ishemia. They found that these circular RNAs contain specific binding sites to target number of domain factors such as TGF- β, apoptosis proteins and multiple miRNA binding sites. Circ_016423 has highest possibility to regulate apoptosis throughout miRNAs via its 625 binding sites (Mehta et al., 2017).

Table 1.1. Circular RNAs reported in apoptosis.

Cell / Tissue Type	Circular RNA	Target	Reference	Pathology
Cerebral Cortex	Circ_016423		Mehta et al., 2017	Transient Focal Ischemia
Umbilical Vein Endothelial Cells	Circ_0010729	miR_186 and HIF1α	Dang et al., 2017	Hypoxia
HEK-293	ANRIL	PES1	Holdt et al., 2016	Atherosclerosis
Mouse Cardiac Myocytes	Cdr1as	miR-7a	Geng et al., 2016	Myocardial Infarction
NCI-H460 and A549	Circ_0043256	miR-1252	Tian et al., 2017	Cinnamaldehyde -induces cell apoptosis
Mouse Neuroblastoma N2a Cells	Circ_Rar1	miR-671	Nan et al., 2016	Lead-induced neuronal cell apoptosis
Rat Endothelial Cells	ANRIL		Song et al., 2017	Coronary Atherosclerosis
Human Aortic Smooth Muscle Cells	Circ_000595	miR-19a	Zheng et al., 2015	Aortic aneurysm
Cardiomyocytes	MFACR	miR-652-3p	Wang et al., 2017	Myocardial Ischemia
66C14, 4T1, MB468 and MB231 Cancer Cell Lines	Circ_Foxo3	MDM2-p53	Du et al., 2017	Stress-induced cell apoptosis

Circular RNA expressions were profiled by microarray technology by using hypoxia-induced human umbilical vein endothelial cells. Thirtysix circular RNAs were identified as differentially expressed significantly. They selected hsa_circ_0010729 randomly among them and validated by qPCR. Loss of function studies indicated that

hsa_circ_0010729 is involved in proliferation and migration as well as apoptosis (Dang et al., 2017).

MTP18 is a nuclear-encoded mitochondrial membrane protein which has a function in mitochondrial fission, as a target of miR-652-3p and its regulation has been attributed to apoptosis-related circular RNA (MFACR) (Wang et al., 2017).

Burd et al. reported circular form of lncRNA ANRIL (Burd et al., 2010). Further, Holdt et al. showed the functions of the circular form of the ANRIL as regulating the maturation of precursor ribosomal RNA and regulating apoptosis in human vascular cells. Overexpression of circular ANRIL in HEK-293 cells led to increase in the apoptosis rate as confirmed by caspase activity, TUNEL assay and qPCR. Additionally, Circular Rar1 was verified by RNA sequencing and qPCR. Mir-671 was shown have affinty for circular Rar1 (Nan et al., 2016).

1.4. Aim

The main aim of the project is to identify differentially expressed circular RNAs via deep RNA sequencing under apoptotic conditions in HeLa cells.

CHAPTER 2

MATERIALS and METHODS

2.1. Cell Culture

HeLa cells were obtained from DSMZ GmbH (Gibco). Cells were cultured in RPMI 1646 supplemented by 10% FBS and 1% penicilin- streptomycin in an atmosphere of %5 CO2 at 37 °C.

HeLa cells were treated with cisplatin, doxorubicin FAS mAB and TNF-alpha ligands. These treatments were performed using 6 well-plate (Sarstedt). 0.3 x 106 cells were seeded per well and incubated overnight. Time- and dose- kinetics experiments were performed in prior studies to obtain significant apoptosis rate in HeLa cells (TUBITAK Project 113Z371). The entire drug treatment experiments were performed in three replicates with their controls. Students's t-test was performed to show statistical significance.

Cisplatin (SantaCruz) was freshly prepared in DMSO as 83.2 mM stock because of its chemical instability. Subsequent experiments were set to 80 μM for 16 hours. DMSO was used as negative control because CP is soluble with DMSO (dimethyl sulfoxide).

Doxorubicin (Cell signalling) was prepared with DNase and RNase free water as 5 mM stock, aliquoated and stored at -20 °C. Experiments were set to 4 μM and 4 hours. Fas mAb (CD95L) (Cell Signalling) was used as concentration of 0.5 μg/ml and 16 hours. TNF-alpha ligands (Millipore) were dissolved in DNase and RNase free water. 100 ng stock was prepared, aliquoted and stored at -20 °C.

Cycloheximide (CHX) (Applichem) was coupled with TNF-alpha because of type II cell feature of HeLa (Miura et al., 1995). CHX was subjected cells were treated with CHX in dose dependent manner to obtain minimum cytotoxic effect. Therefore; experiments were set to 125 ng/ml TNF-alpha with 10 μg CHX for 8 hours. Cycloheximide alone and TNF- alpha alone were used as negative control.

2.2. Apoptosis Measurement

Three replicates of drug treatment experiments were analysed with MUSE cell analyser (Milipore). Annexin V and 7AAD (BD) were used in apoptosis detection. Dilution rates were 1:5 and 1:10 for Annexin V and 7AAD, respectively. Both of them were diluted with 1X PBS. Ice cold 1X PBS was used to wash drug treated and control cells, after harvesting with Trypsin-EDTA (Gibco, 0.25%). After PBS washing, 50 µl 1X annexin binding buffer (BD) was used to dissolve cell pellets, followed by labelling with 10 µl of Annexin V and 7AAD. Cell pellets were incubated 15 min in dark. After addition of 150 µl 1X PBS, analysis was performed. Annexin V positive cell population was considered to be the early apoptotic cells. Both Annexin V and 7AAD positive cell population was considered as the late stage of apoptosis. 7AAD positive and Annexin V negative cell population was regarded as death cells. Live cells were 7AAD and Annexin V negative.

2.3. Deep RNA Sequencing

Cell lysates from three replicates of four drugs with untreated control cells were sent to deep sequencing by NOVAGENE (Hong Kong). Total RNAs from cisplatin, doxorubicin, TNF-alpha and Fas mAb trated cells and control cells were isolated by NOVAGENE. RNA seq was performed using a specific method based on circular RNA identification (Szabo et al., 2016).

2.4. Bioinformatic Analyses

Circular RNAs were identified by NOVAGENE and were sent with their cirbase ID. (Hong Kong). 10 different candidates were chosen based on differential expression results (CP vs DMSO, TNF vs DMSO, FAS vs DMSO and DOX vs DMSO). All differentially expressed circular RNAs were classified based on their fold change, pathway-drug specificity and source genes. The mRNAs they originated from was sorted as well as. Potential miRNA binding sites of our candidates were identified from RNA-seq data. The involvement of these potential miRNAs in apoptosis were found from

literatüre search. To determine potential Cl, CircInteractome web tool, CPAT (Coding potential assesment tool), Ensembl and IRESite: The database of experimentally verified IRES structures were used. CircInteractome tools provide information about RBPs (EIF4A3). According to previous studies circularRNAs originating first exon of original genes have more coding potential than others (Pamudurti et al., 2017). Sequences of genes which produce our candidate circular RNAs were examined by using Ensembl and candidate circular RNAs that contains 1st exon sequences of original transcript were identified.

For all candidates, divergent primers were designed by using the CircInteractome web tool (Dudekula. et. al., 2016). These primers were specific to amplify backsplicing junctions of candidate circular RNAs, excluding the potential fort he amplification of lineer mRNAs.

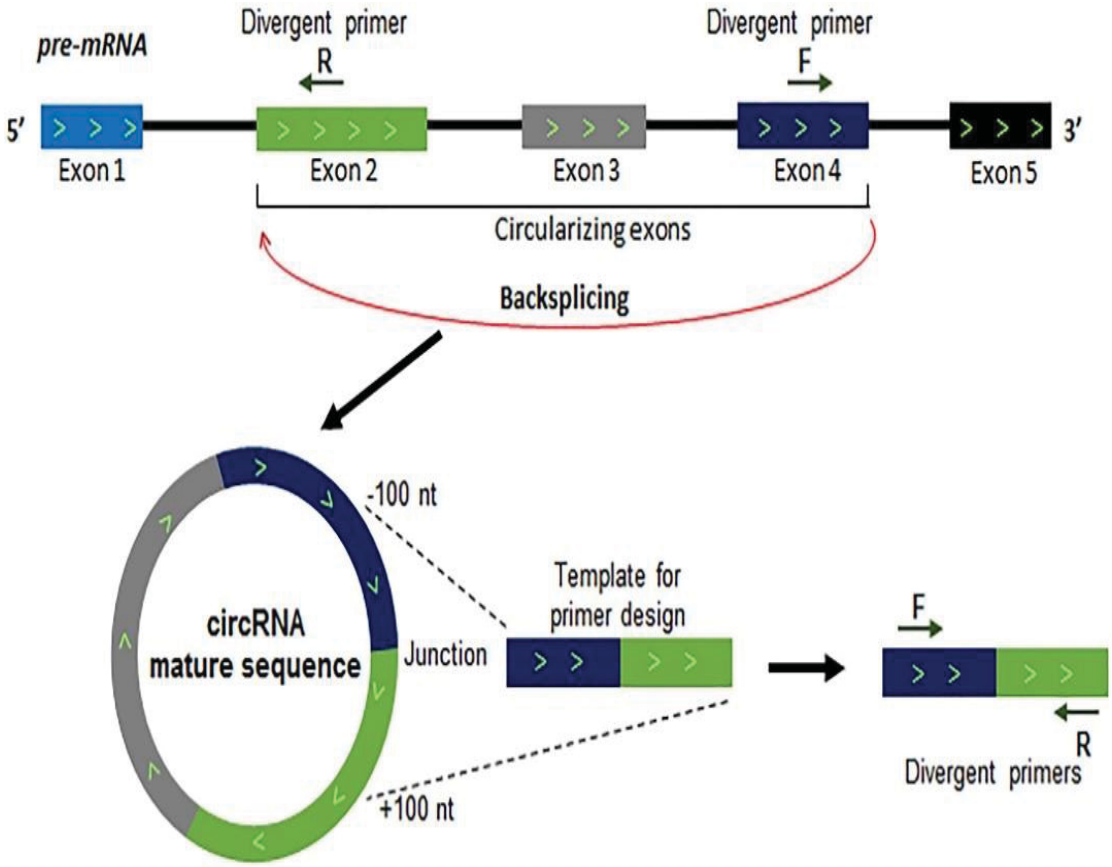

Fig 2.1. Schematic illustration of circular RNA biogenesis from backsplicing of pre-mRNA and divergent primer designing by using the circular RNA junction as template for amplification. (Source: Panda et al., 2018)

2.5. Total RNA Isolation

Cells were grown in 75 cm^2 flasks before treatment. Drug treated and DMSO control cells were harvested with Trypsin-EDTA. Further cells were then washed with cold PBS twice. 1 ml TRizol reagent (Life Technologies) was added into eppendorfs in order to dissolve each pellet after all PBS was removed completely. RNA isolation was carried out by following the protocol from manufacturer.

After TRizol reagent addition, samples were incubated 5 min at room tempature after complete dissociation. Homogenization of each samples were carried out by adding 200 µl RNase free chloroform (Sigma). Samples were shaken vigorously by hand for 15 sec and incubated for 3 min at room tempature. All samples were centrifuged at 12,000 x g for 15 min at 4°C to obtain aqueous phase. After centrifugation aqueous phase was drawn from top by angling the tube at 45° to avoid contaminate upper phase contains RNA with middle or bottom phase. Each sample were treated 0,5 ml RNase free isopropanol (Sigma) and incubated 10 min at room tempature. After that, samples were centrifugated at 12,000 x g for at 4 °C and supernatant was discarded carefully. One ml of %75 RNase free Ethanol (Sigma) was used for washing twice. After pipetting, samples were centrifugated at 7,500 x g for 5 min at 4 °C twice and supernatant was removed after. Pellet samples were left to air. Further, pellet was dissolved with RNase DNase free water and kept -80 °C until use.

RNA quantity and quality were checked by both NanoDrop (Thermo Scientific) and %1 agarose gel electrophoresis, respectively. Pure RNA should have ~2 as 260/280 and 260/230 ratio. RNAs were loaded onto 1% agarose gel and was run in TBE buffer (Tris-borate-EDTA buffer, 890mM Tris-borate, 890mM boric acid, 20mM EDTA.) for 25 min at 100V. After running, the gel was visualized for 10 sec under UV light via AlphaImager (Model IS-2200, AlphaImager High Performance Gel Documentation and Image Analysis System).

2.6. RNAse R Treatment for CircRNA Enrichment

RNAse R (Epicentre) was applied to both cisplatin treated and untreated control RNA to eliminate linear RNA and to enrich for circular RNA. Inıtially RNA quantity was measured by NanoDrop and 2 µg of prepared RNA, 1 µl buffer, 0.25 µl RNase R enzyme

and variable amount of RNase DNase free water were mixed up to 10 µl final volume and incubated for 30 min at 37 °C. After that RNA clean up from reaction mixture was performed with Nucleospin RNA kit (MN). Initially, volume of RNA samples were completed to 500 µl with RNAse free water. The resulting solution was mixed with 6 volumes of equal amounts of Buffer RA1 and Ethanol (For 500 µl of RNA solution, 1,500 µl of Buffer RA1 and 1,500 µl of Ethanol). Further, mixtures were loaded into NucleoSpin® RNA Column and centrifuged for 30 sec at 11,000 x g. Columns were washed with 200 µl Buffer RAW2 by centrifugation for 30 sec at 11,000 x g. Likewise, 600 µl and 250 µl Buffer RA3 was used for washing twice, respectively. Samples were centrifuged for 30 sec followed by 2 min at 11,000 x g. RNAse R treated RNA samples were centrifuged for 1 min at 11000 x g and eluted via 40 µl RNAse free H2O.

2.7. cDNA Synthesis and PCR

cDNAs were prepared with the following samples: RNAse R treated CP and DMSO, non-treated CP and DMSO. Proportionally 1 µg RNA, 2 µl random primer, 10 µl M-MuLV reaction mix, 2 µl M-MuVL enzyme mix (NEB) and variable volume of RNase DNase free water to final volume 20 µl were mixed. Due to random primer usage we used 5 min prior incubation at 25°C. Further, mixtures were incubated for 1 hour at 42°C followed by incubation at 80°C for inactivation of enzyme. After sample dilution, Taq Polymerase (NEB) was used to verify backsplicing junction of circular RNA candidates and circular RNA control. PCR conditions were as follows: Initial denaturation at 95 °C for 30 sec, 35 cycle of denaturation at 95°C for 30 sec, annealing at 60°C for 1 min, extention at 68°C for 1 min, 1 cycle of final extention at 68°C for 5 min.

2.8. Validation of Circular RNAs by Cloning

Bands of the correct size were cut from the gel for DNA extraction by gel extraction kit (MN). Firstly, 200 µl Buffer NT1 was added for each 100 mg of agarose gel. Samples were incubated at 50 °C for 5-10 min. After complete dissolution, samples were loaded onto NucleoSpin® Gel and PCR Clean-up Column and centrifuged for 30 sec at 11,000 x g. Following centrifugation, 700 µl buffer NT3 was added to the column

and centrifuged for 30 sec at 11,000 x g. Flow through was discarded and silica membrane was dried via centrifuge for 1 min at 11,000 x g.

Finally, DNA samples were eluted into a 1.5 ml eppendorf by adding 30 µl buffer NE after incubation at room tempature for 1 min. Columns were centrifuged for 1 min at 11,000 x g. Adenylation was performed with the help of Taq polymerase for TA cloning of ThermoScientific. Twelve µl extracted DNA, 0.4 µl dATP, 2 µl MgCl free standard Taq buffer, 1.2 µl MgCl, 0.125 µl Taq polymerase were mixed in a total volume of 20 µl volume and the mixture was incubated at 72°C for 20 min.

Cloning was performed by using TA Cloning Kit (with pCR II Vector) (Thermoscientific). 2 µL 5X Express Link™ T4 DNA Ligase Buffer, 2 µL pCR®II vector (25 ng/µL), 1 µL ExpressLinkTM T4 DNA Ligase (5 units) and 5 µL of extracted DNA were mixed and incubated at room tempature for 15 min. DH5α competent bacteria were used for transformation. 2 µL plasmid (with insert) and 20 µL of competent bacteria were mixed and incubated 20 min on ice.

Further, cells were heat schocked at 42°C for 50 sec and placed on ice immediately for 2 min. SOC (900 µL) medium was added onto transformed bacteria and incubated at 37°C for an hour. After incubation, bacteria were centrifuged at 5,000 x g for 30 sec and supernatant was discarded. Finally, transformant bacteria were spread on plates with ampicillin (100 mg/mL) which contains IPTG (0.1 mM) and X-gal (40 ug/ml). White colonies were selected and transferred into small scale LB culture for 16 hours.

MiniPrep (MN) were carried out with a single colony. Saturated LB culture was centrifuged for 30 sec at 11,000 x g. Pellet was resuspended by addition of 250 µL buffer A1. After resuspension, 250 µL buffer A2 was added and samples were incubated at room tempature for lysis. Neutralisation was performed with 300 µL buffer A3 and incubated until samples turn colorless. Samples were centrifuged at 11,000 x g for 5 min for clarification and supernatant was transferred onto NucleoSpin® Plasmid/Plasmid (NoLid) Column. Columns were centrifuged for 1 min at

11,000 x g and flowthrough was discarded. Silica membranes were washed with 500 µL buffer AW and 600 µL buffer A4 and centrifuged for 1 min at 11,000 x g. Silica membranes were dried by centifugation for 2 min at 11,000 x g. Finally plasmid DNA was incubated with 50 µL buffer AE for 1 min and eluted by centrifugation for 1 min at 11,000 x g. Plasmids were sequenced by BIOMER (IYTE) to validate the backsplice junction of target circular RNAs.

2.9. Quantitative PCR

GoTaq q-PCR Master Mix (Promega) was used for q-PCR reactions (Roche lightcycler 96). 12.5 µl GoTaq q-PCR Master Mix, 9 µl DNase RNase free water, 1 µl primer mix (25 mM) and 2.5 µl template DNA were used for one reaction in a volume of 25 µl. Cisplatin treated and untreated control goups serve as template of qPCR. Two step PCR amplification conditions were as follows: initial denaturation at 95 °C for 2 min, (40 cycle) denaturation at 95°C for 15 sec and annealing/extention at 60°C for 1 min.

CHAPTER 3

RESULTS

3.1. Apoptosis Rates of Drugs, RNA Isolation and Quality Control

DMSO (0.1 %) was used as control group and incubated for 16 hours. Cisplatin (CP) dose was 80 µM and it was incubated for 16 hours. HeLa cells were treated with Anti Fas/CD95 (0.5 µg/ml) , doxorubicin (0.5 µM) for 16 hours and 4 hours, respectively. TNF-alfa (0.125 ng/ml) and CHX (10 µg/ml) was applied for 8 hours. As a result of TNF-alpha is functional in CHX existence. HeLa cells were treated with only CHX as a control. CP, DOX, TNF-alfa and FAS ligand caused 24.67%, 25.83%, 33.57% and 13.77% of apoptosis, respectively. All values were obtained as three replicates.

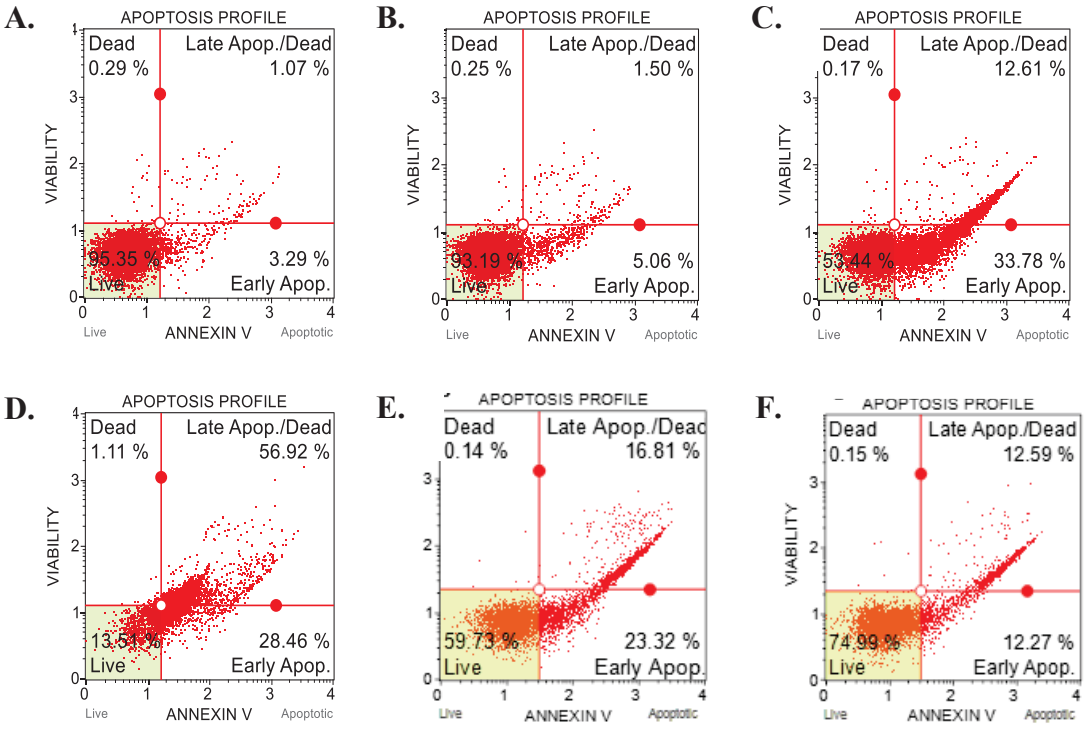

Figure 3.1. Flow Cytometry profiles of one replicate of each. A. DMSO control, B. CHX, C. TNF-alpha, D. DOX, E. CP and F. FAS screening via Annexin V and 7AAD staining. Live cells were Annexin V-/7AAD- ; dead cells were Annexin V-/7AAD+; apoptotic cells were Annexin V+/7AAD-.

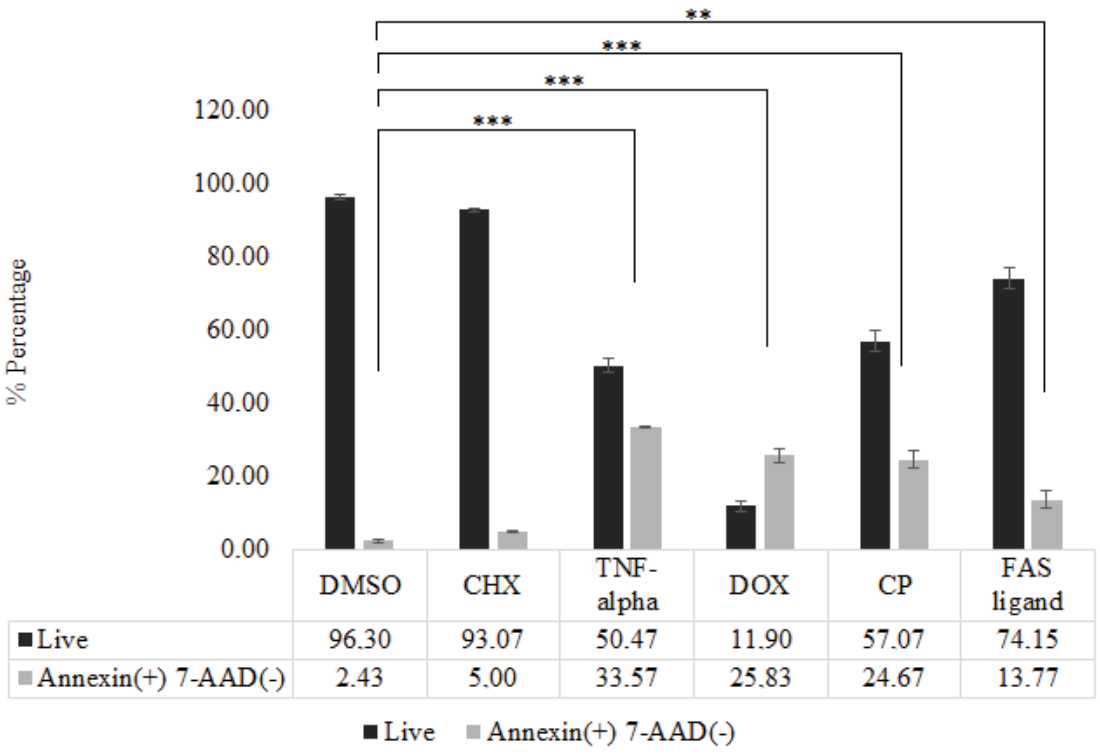

Figure 3.2. Apoptosis induction in HeLa cells. Statistical analysis was performed by student's t test. P<0.05. p<0.001 (***), p<0.01 (**).

Total RNAs from drugs treated cells were first run on a 1% agarose gel. 28S and 18S rRNA were visualized to track quality.

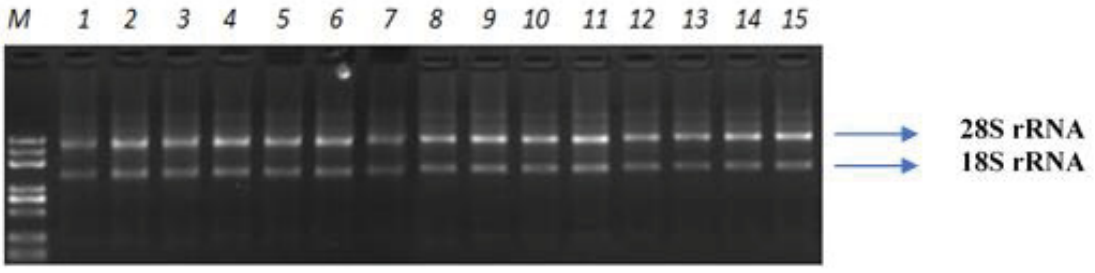

Figure 3.3. RNA gel and quality check (QC) analysis of total RNAs. Agarose gel (1%) shows integrity of 3 replicates of RNA which were isolated from each control(1,2,3), TNF-alpha (4,5,6), Doxorubicin (7,8,9), Cisplatin (10,11,12) and FAS (13,14,15) treated HeLa cells.

3.2. Bioinformatic Analysis of Circular RNA Candidates

The original raw data from high throughput sequencing (illumina HiSeqTM2500) which consisted of raw pictures were first transformed to Sequenced Reads containing reads sequence and corresponding base quality (in FASTQ format) through Base Calling. Novel circRNAs were identified and annotated by CIRCexplorer (Xiao-Ou Zhang et al., 2014), which remapped the unmapped reads to the genome by tophat's fusion-search to find back-spliced reads. The normalized expression of circRNAs in each sample was calculated based on the TPM (Zhou et al., 2010) method. The input data was the readcount value from the expression level analysis of circRNA. For samples with biological replicates, DESeq2 (Michael et al., 2014) was used to performed the analysis. For the samples without biological replicates, TMM was first used to normalize the read count value, and the DEGseq (Wang et al., 2010) was used to do the analysis (Figure 3.4)

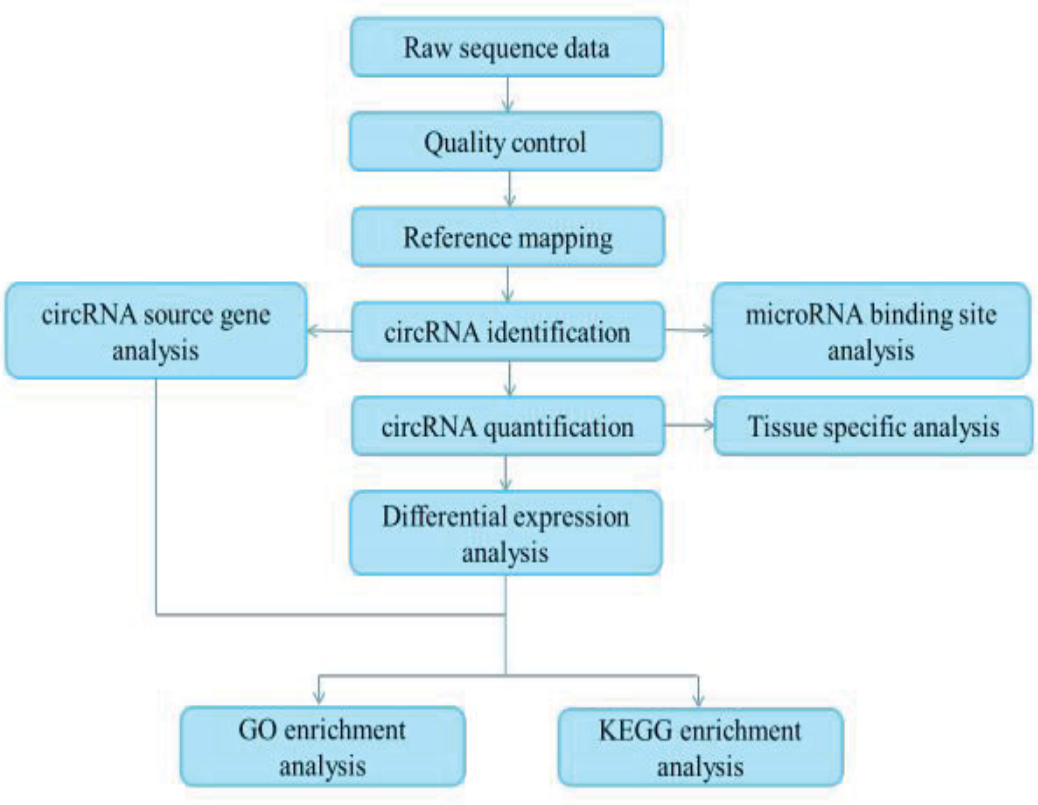

Figure 3.4. The procedure of circRNA-Seq analysis.

TPM cluster analysis results indicated that circular RNA expression differences among control group and drugs. Huge discrepancy exist between TNF-alpha and DMSO control group. Likewise, CP caused differential trend in a variety of circular RNAs. However, number of circular RNAs differentially expressed in DOX and FAS treated HeLa cells was remained limited (Figure 3.5).

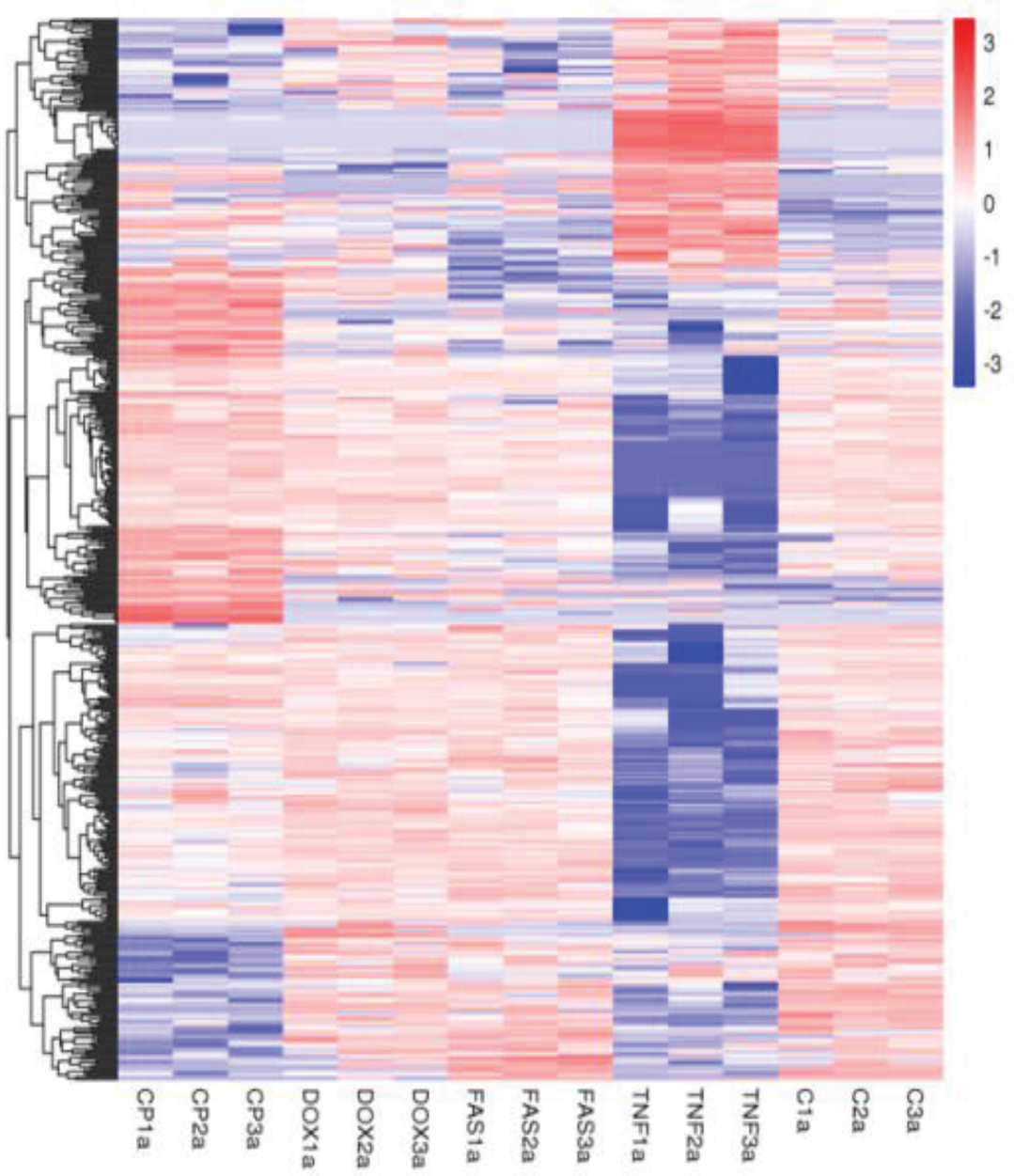

Figure 3.5. The overall TPM cluster analysis result. Clustering is based on log10(TPM+1) value, red represents circRNAs with high expression level, blue represents circRNAs with low expression level. The colour from red to blue represents the log10(TPM+1) value from large to small.

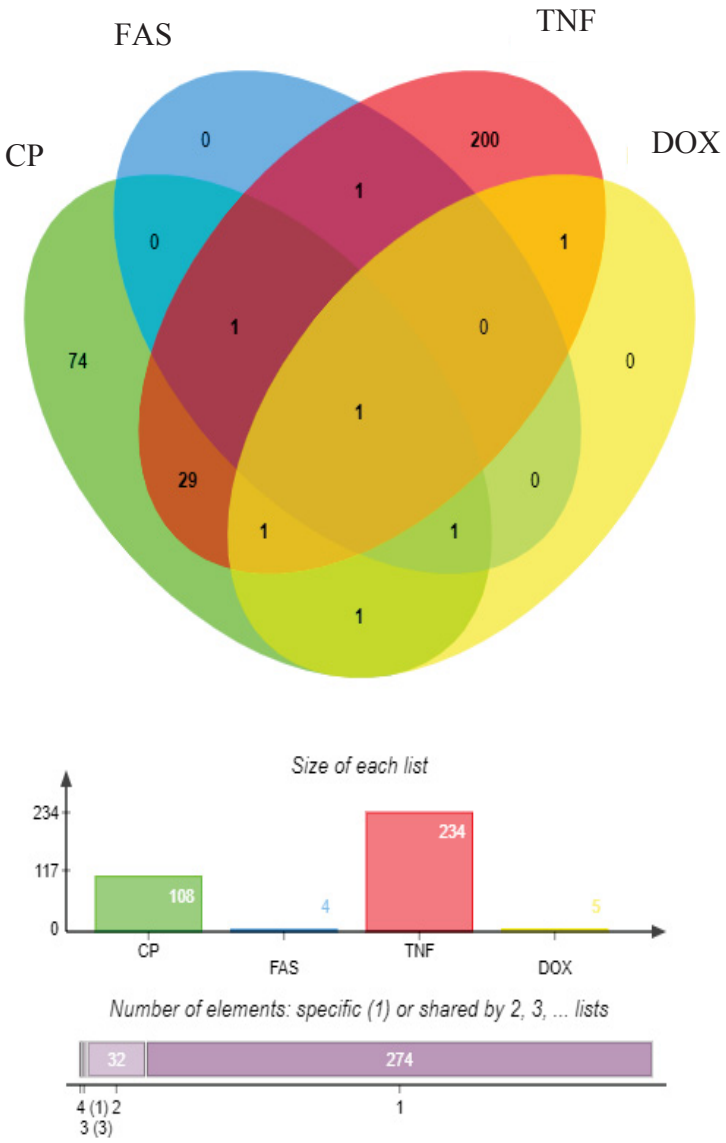

Figure 3.6. Distribution of circular RNA candidates differentially expressed in apoptotic HeLa cells. CP, cisplatin; Fas ligand, TNF-alpha and DOX, doxorubicin.

Venn diagram shows that 108 circular RNA were differentially expressed in CP treated HeLa cells. Likewise 234 circular RNA showed differential expression in TNF-alpha treated HeLa cells, significantly. Five and four circular RNA were differentially expressed in DOX and FAS treated HeLa cells, respectively. Candidate-2 is the only candidate differentially expressed in each of drugs. Candidate-1 shows significant expression differentiation under CP, DOX and FAS ligand treatment. TNF-alpha and CP triggered differential expression of drug spesific 200, 74 circular RNA, respectively (Figure 3.6).

Table 3.1. Circular RNA candidates differentially expressed in apoptotic HeLa cells. Circular RNAs that were significantly down- and up-regulated upon treatment with all agents is listed below with their parental coding mRNAs. The majority of top 5 upregulated and downregulated circular RNAs are originated from protein coding genes well-documented to regulate apoptosis. The microRNAs were chosen as targets based on binding site analysis to investigate circRNA-mediated sponging of miRNAs. Apoptosis related miRNAs, let -7 family, hsa-miR-106a-3p, hsa-miR-103a-3p, hsa-miR-106a-5p were common in all candidates. P-value, log change and apoptosis relation of parental genes were considered as criteria to choose candidate circular RNA.

Circular RNA	**P-val**	**Log change**	**Parental mRNA**	**miRNA binding sites**
Candidate-1	2.29E-04	71.045	FGF14	hsa-let-7d-3p hsa-miR-103a-3p hsa-miR-106a-5p
Candidate-2	0.00053703	50.376	XPO7	hsa-let-7c-5p hsa-let-7d-5p hsa-let-7e-5p
Candidate-3	0.00068894	49.662	STAT5A	hsa-let-7a-2-3p hsa-miR-101-3p
Candidate-4	0.0004384	50.975	BBC3	hsa-let-7c-3p hsa-miR-106a-3p
Candidate-5	9.18E-01	55.021	ARHGEF11	hsa-let-7f-2-3p hsa-miR-103a-3p
Candidate-6	0.00038011	-36.338	LATS2	hsa-miR-103a-2-5p hsa-miR-106a-5p
Candidate-7	0.00039188	-36.291	TRRAP	hsa-miR-105-3p
Candidate-8	0.00014162	-53.499	USP33	hsa-let-7a-2-3p
Candidate-9	0.00011961	-53.925	PTPN12	hsa-let-7a-2-3p
Candidate-10	0.0001054	-54.228	TMEM132C	hsa-let-7a-2-3p

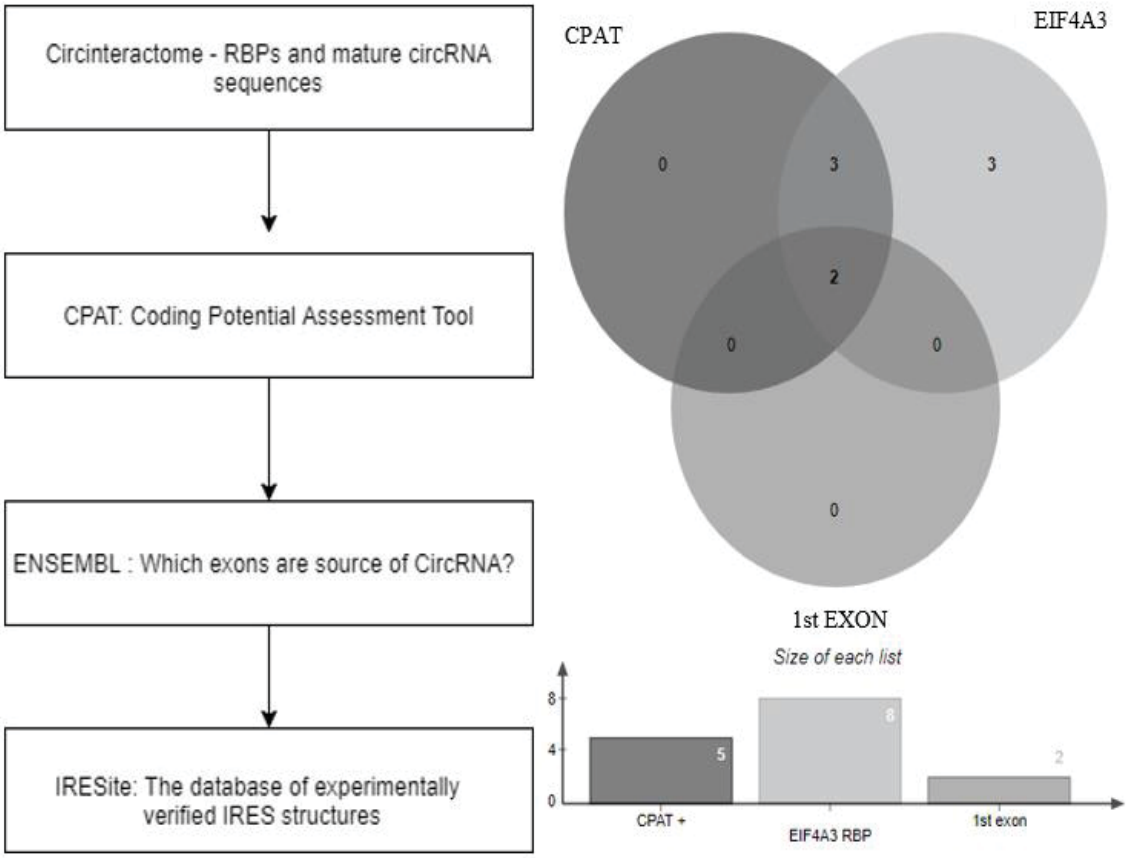

Figure 3.7. Workflow of coding potential analysis of circular RNA candidates.

Criteria in candidate selection were log change among drug treated and control groups, statistical significance of differential expression and potential involvement of parental genes in apoptosis. Candidate-1, candidate-2, candidate-3, candidate-4 and candidate-5 were upregulated under apoptotic conditions. Rest of them were downregulated. All the candidates showed differential expression via CP treatment. hsa-let-7, hsa-miR-103, hsa-miR-105, hsa-miR-101 and hsa-miR-106 are common with regards to existance of miRNA binding sites in circular RNAs (Table 3.1.).

Circinteractome (Dudekula DB et al., 2016) was used in order to obtain sequences of mature circular RNA candidates and find possible RBP interactions. After that, coding potential assessment tool was utilized to investigate their coding probability (Wang et al., 2013). According to literature, circular RNA which is originated from the first exon of parental gene has a high coding potential (Pamudurti et al., 2017). Thus, all candidates source exons were screened via ENSEMBL (Zerbino et al., 2018). Finally possible

internal ribosome entry site (IRES) sequences in our candidates were searched via IRESite database (Mokrejš et al., 2006), because circular RNA can be translated by cap-independent way (Legnini et al., 2017). These analyses showed that Candidate-6 and candidate-4 exhibited the highest possibility for translation (Figure 3.7).

3.3. Validation of RNAse R Treatment

RNAs were isolated from three biological replicates of CP treated HeLa cells and DMSO control groups. RNAs were first measured via spectrophotometer then were run in a 1% agarose gel. Based on 260/280, 260/230 ratios and gel bands, RNAs were pure and intact.

Circ-HIPK3 was chosen as a positive control to optimize circular RNAvalidation. Li et al. reported that Circ-HIPK3 was expressed in HeLa cells (Li et al., 2017). Divergent primers were designed via Circinteractome tool (Dudekula et al., 2016). qPCR was performed with cDNAs that were reverse transcribed from both RNAse R positive and negative samples (Figure 3.8).

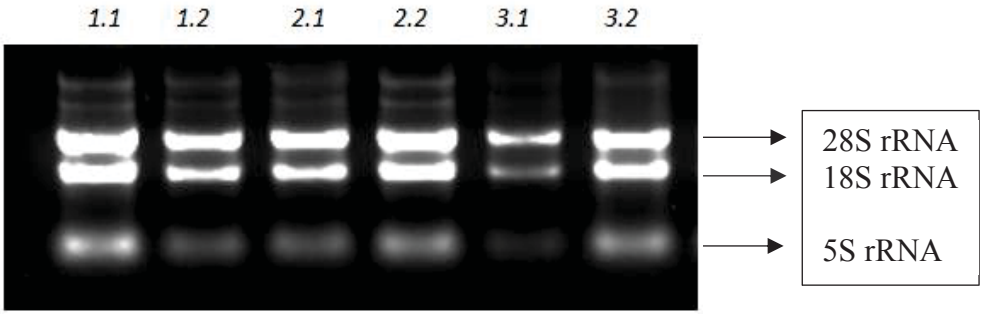

Figure 3.8. RNA Gel and Quality Check (QC) Analysis of Total RNAs. Total RNAs of apoptotic HeLa cells (1.1, 2.1, 3.1) and DMSO (2.1, 2.2, 2.3) control group were running at 90 V for 30 min.

As expected circ-HIPK3 expression was not affected by RNAse R treatment, however, Cq values of GAPDH increased dramatically because of its linearity. Results indicate that, amount of circ-HIPK3 did not change (0<cq change<1) in both CP and DMSO treated samples, but amount of GAPDH decreased approximately 222 fold in RNAse R treated samples (Figure 3.9).

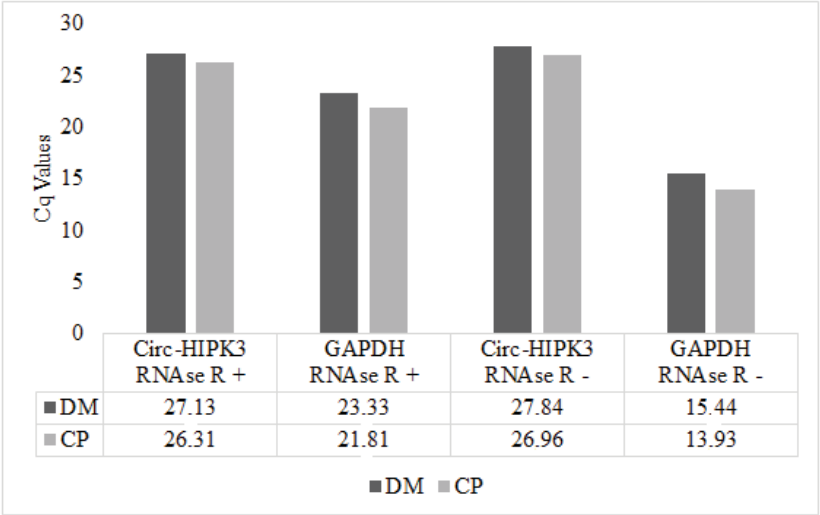

Figure 3.9. Quality control of RNAse R treatment of CP and DMSO treated RNA by qPCR. One sample was used for QC. Circ-HIPK3 was used as circular RNA and GAPDH was as linear control.

RNAse R treated DMSO group was used as template for backsplicing junctions of candidates in traditional PCR. Circular RNAs showed resistance to RNAse R mediated degredation unlike linear RNA transcripts. Beta actin was used with both RNAse R positive and negative DMSO (DM) groups.

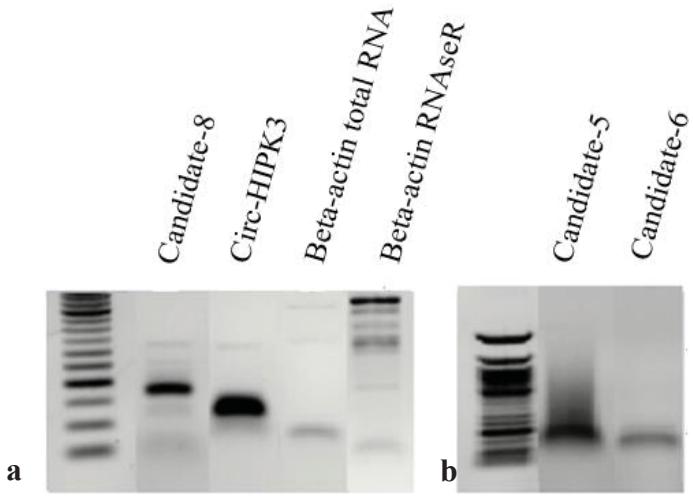

Figure 3.10. Agarose gel (1%) image shows backsplicing junctions of circular RNA candidates. (a) Candidate-8 and circ-HIPK3 was shown and beta actin was used with both RNAseR positive and negative samples. (b) Candidate-5 and candidate-6 were indicated.

Backsplicing junction of candidate-8, circ-HIPK3, candidate-5 and candidate-6 were validated in RNAse R treated RNA. RnaseR treated samples were used as template to show circularity of our product. PCR conditions were optimized for qPCR. Beta actin was used as positive control to confirm success of RNAse R treatment and linear RNA degredation. Beta actin was used in RNAse R negative sample to confirm that PCR was working and RNAse R negative cDNA works well.

3.4. Validation of Circular RNAs by Cloning

According to the CirBase, Circ-HIPK3 was originated from 1099 bp exon of HIPK3 gene (Zheng et al., 2016). After extraction of circ-HIPK3 band from agarose gel (Figure 3.10.b), sample were subjected to sequencing. Results showed that amplified band belongs to backsplicing junction of circular-HIPK3 (Figure 3.11)

a

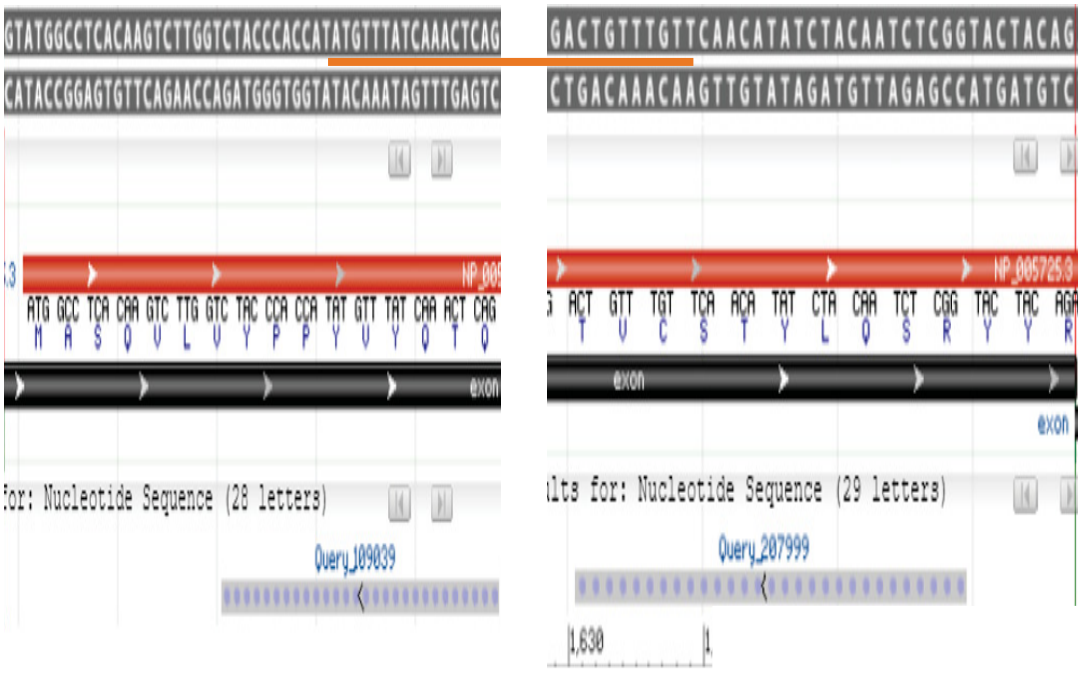

Figure 3.11. Validation of circ- HIPK3 by cloning. (a) Blast search of divergent primers of circ-HIPK3, matching with to two tail of 1099 bp exon. (b) Sequencing results indicated backsplicing junction of circular-HIPK3.

(Cont. on next page)

b

GAATTCGGCTTCTGAGTTTGATAAACATATGGTGGGTAGACCAAG
ACTTGTGAGGCCATACCTGTAGTACCGAGATTGTAGATATGTTGA
ACAAACAGAAGCCGAATTC

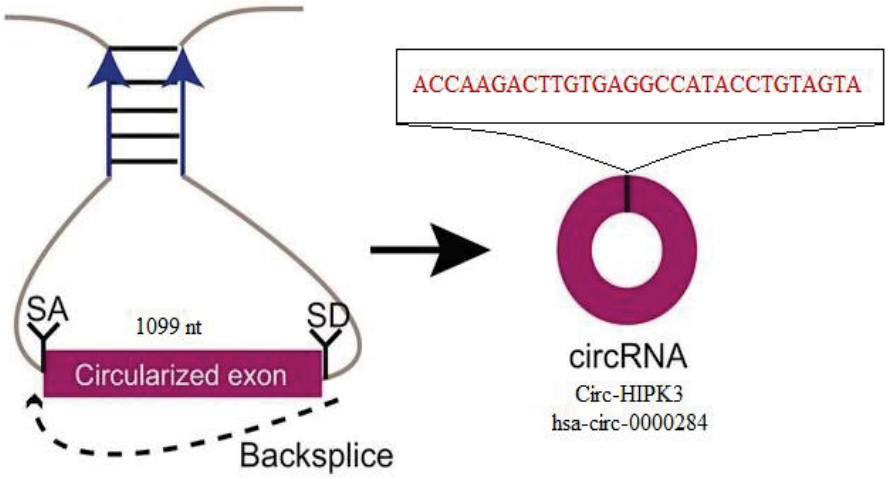

Figure 3.11. (cont.)

Circ-HIPK3 derived from second exon of HIPK3 gene. The genomic structure shows that circHIPK3 contains a large second exon (1,099 bp) from the HIPK3 gene flanked by long introns on either side. The distinct product of the expected size was amplified using outward-facing primers and confirmed by sequencing (Figure 3.11). BLAST analysis shows that divergent primers matched with two tails of the second exon of HIPK3 gene and gave back splicing junction sequence of circ-HIPK3. Sequencing indicates that PCR product (Figure 3.10) belongs to backsplicing junctionof circ-HIPK3 which is not exist in linear form of HIPK3 mRNA.

3.5. Quantitative PCR

Circ-HIPK3 was downregulated in CP treated samples by 2.53 fold and candidate-8 was downregulated in CP treated samples as 3.44 fold (Figure 3.12 and Figure 3.13). Candidate-6 was upregulated in apoptotic HeLa cells as 5,9 fold (Figure 3.14).

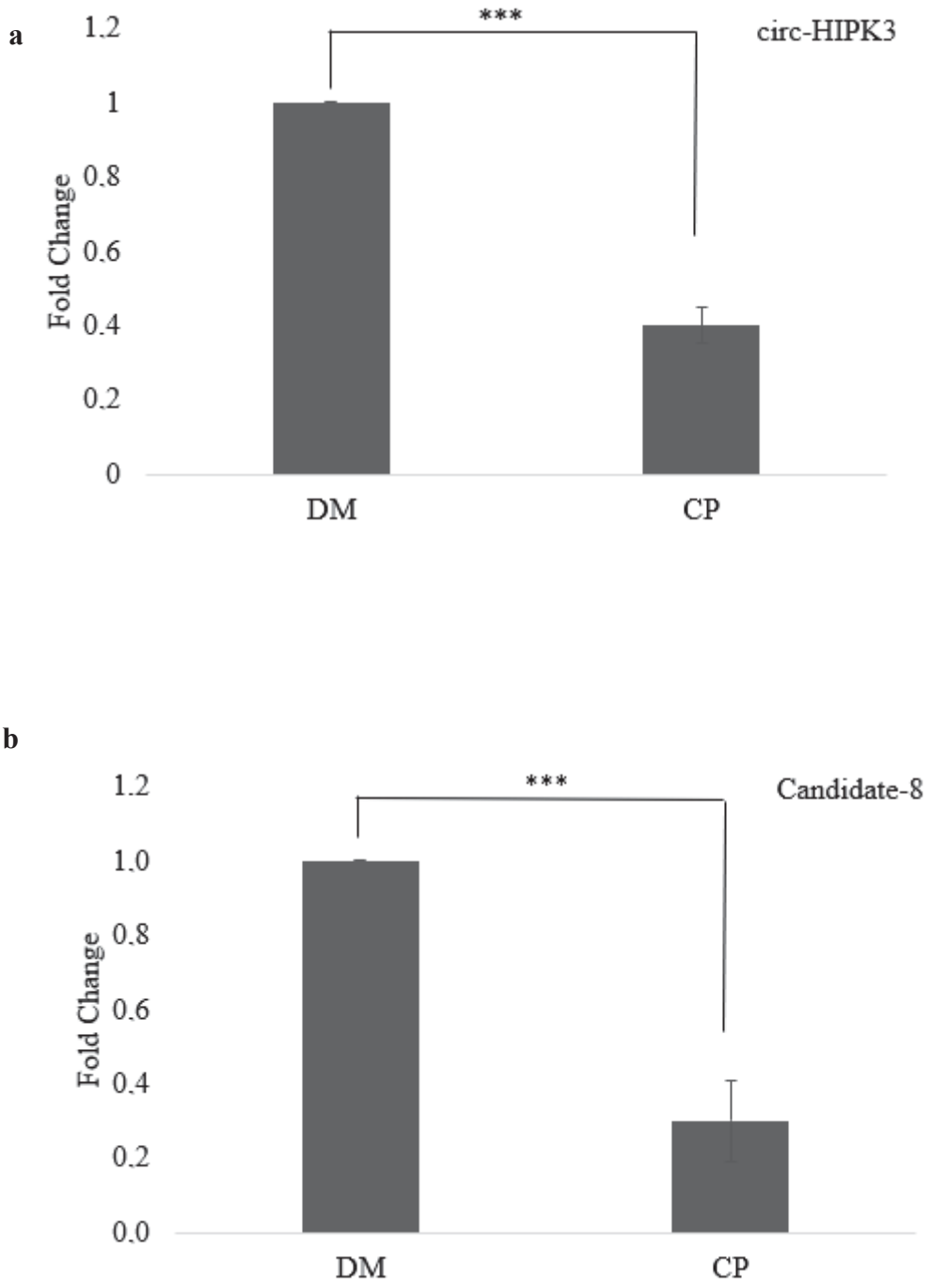

Figure 3.12. qPCR analysis of (a) circ-HIPK3, (b) candidate-8 and (c) candidate-6 expression. Statistical analysis was performed by Student's t test. p=6,111E-05 (circ-HIPK3), p=0.0007 (candidate-8), p= 0.03 (candidate-6). p<0.05 (*), p<0.01 (**), p<0.001 (***).

(Cont. on next page)

c

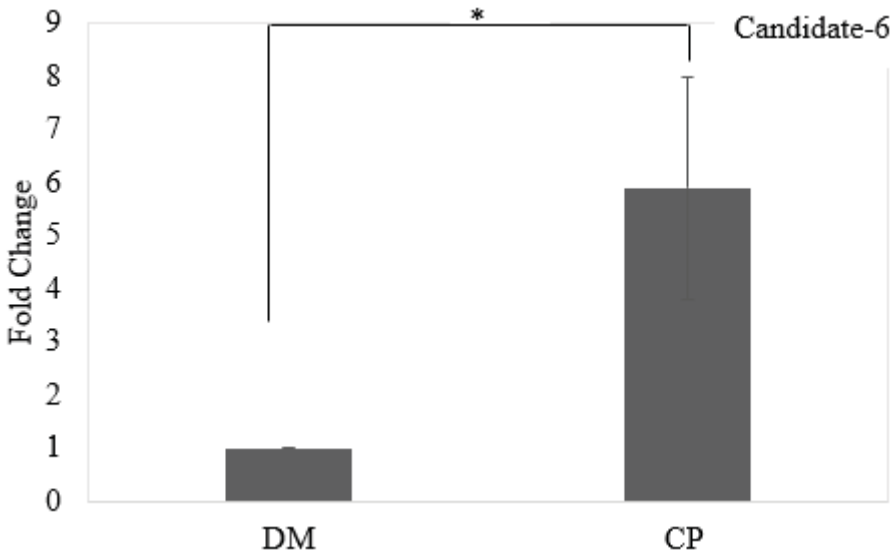

Figure 3.12. (cont.)

CHAPTER 4

DISCUSSION

Circular RNA research is a quite new and hot topic in the field of RNA biology and detection of circular RNAs by sequencing is still challenging. Basically, circular RNAs can be detected by RNAseq to identify sequence reads spanning backsplicing junctions which do not colinearly map to the referance genome. (Gaffo et al., 2018) False-positivity of splice site identification is still a major problem, and bioinformatical improvements are needed to improve accuracy. Besides, rRNA and poly-A depletion are valuable approaches used for the enrichment of circular RNAs in sequencing. It is not certain that the enriched sequences are exclusively circular due to the presence of non-coding RNAs.

The overall TPM cluster analysis result indicated that TNF-alpha causes differential expression of 234 circular RNAs as compared with DMSO control group. Likewise, cisplatin also showed oppossite expression profile as compared with DMSO control group, but not sharp like in TNF-alpha. Doxorubicin and FAS caused less number of differentially expressed circular RNAs circular RNAs, nearly 2% of TNF-alpha. Profile differences of TNF-alpha and cisplatin compared to doxorubicin and FAS in terms of circular RNA expression remains questionable. In the light of RNA- seq results, three different circular RNA expression pattern of four drugs can be determined clearly. TPM cluster results of cisplatin and TNF-alpha suggest that circular RNAs differentially expressed in TNF-alpha treated apoptotic HeLa cells are also nearly 80% different from cisplatin treated apoptotic HeLa cells. This difference might be originated from drug-pathway specification, due the fact that TNF-alpha triggers extrinsic apoptotic pathway but, cisplatin effects intrinsic apoptotic pathway.

Candidate circular RNAs were selected based on the extend of their differential expression rate. Totally ten candidates and one positive control were selected. Firstly, we needed to optimize circular RNA detection methods because of the experimental challenges of detecting circular RNA (Szabo et al., 2016). Therefore circ-HIPK3, which was reported in HeLa cells previously (Zheng et al., 2016), was chosen as positive control. Candidate-1 was selected due to increased expression under all of four drug treatments,

dramatically. Likewise, expression of candidate-2 significantly increased in TNF-alpha, cisplatin and fas-ligand treated populations. Further, 5 top candidates per upregulation and downregulation list off all drugs were classified. Remaining eight candidate were performed with cisplatin treatment, because further wet lab experiment were performed with cisplatin treatment. Source genes of candidates and possible miRNA binding sites were analysed. Most common binding site of all of ten candidates is hsa_let_7 and hsa_miR_106, which are commonly involved in apoptosis (Zhang et al., 2013; Qin et al., 2018). They might modulate apoptosis through sponging hsa_miR_let_7 and hsa_miR_106. However, circular RNAs might be functionally independent from its parental gene or have an effect on its parental gene function (Barrett et al., 2016). One of our candidates namely candidate-4 is originated from BBC3 (BCL2 Binding Component 3), which was also known as the p53 upregulated modulator of apoptosis (Belle et al., 2016). Huang et al. reported that lots of ciRNA regulate gene expression in *cis*. Some well characterized ciRNAs namely ci-sirt7 and ci-ankrd52 accumulate in nucleus and associate with the elongated RNA Polymerase II complex. Decrease for RNA in cells reduce the transcription level of their parental genes ANKRD52 or SIRT7. Therefore, it can be suggested that circular RNAs promote pol II transcription of parental genes, however, mechanism of action is unknown. In our cases, candidate-4 might promote BBC3 gene transcription level. BBC3 associate with, inactivate anti-apoptotic bcl-2 member, and promote apoptosis (Krishna et al., 2011). Besides, coding probability of candidate-4 is higher than remaining, as originated from first exon of its parental gene and it contains methylation site on upstream of AUG. Candidate-3, is originated from STAT5A, which is involved in anti-apoptotic pathways (Kaymaz et al., 2013). Transcription level of STAT5A might be regulated negatively by candidate-3 through RNA splicing competition or RNA polII binding mechanism. Candidate-5 is originated from ARGHEF11, which is involved in c-jun N-terminal kinase-mediated apoptosis (Harrington et al., 2002). Parental gene of candidate-6 is LATS2 which is a tumor suppressor and induces apoptosis by downregulation of Bcl-2 and Bcl-x(L) (Ke et al., 2004). Parental genes of other candidates are not related with apoptosis, but as mentioned circular form of linear mRNAs might have very different function. According to RNA-seq, they exhibited differential expression, dramatically. Therefore, they should be checked.

RNA isolation from CP treated cells was performed to validate positive control circular RNA and our candidates. CP was chosen rather than TNF-alpha for further

experiment because CP caused consisant cell death and can be used much easier than TNF-alpha, which needs CHX to induce apoptosis. Thus, CP is suitable for initial validation of selected candidates. After that drug spesific profiles will be searched.

Beta-actin was used as linear housekeeping control. RNAse R treatment was performed to deplete linear transcripts and enrich circular RNA. We designed divergent primer to amplify backsplicing junction specifically. Circular RNA abundance was extremely low as compared with linear counterparts (Szabo et al., 2016). Normally, PCR reaction should not produce linear form of circular RNA, but primers might be sponged by parental gene. Thus, we were not be able to show circular RNAs in PCR without RNAse R treatment. Quality control of RNAse R treatment was done via qPCR by using circ-HIPK3 and GAPDH. As expected, cq values of circ-HIPK3 did not change, but cq values of linear GAPDH increased dramatically (Figure 3.9).

Circ-HIPK3, candidate-8, candidate-5 and candidate-6 were shown via RNAse R treated RNA sample (Figure 3.10). Beta actin was used as control of both RNAse R treated and non-treated template to confirm depletion of linear transcripts. There was no beta actin in RNAse R treated sample unlike mock control RNA. On the other hand, clear bands of Circ-HIPK3, candidate-6, candidate-5 and candidate-8 were visualized, referring to presence of circular RNA in HeLa cells (Figure 3.10).

We performed TA cloning and sequencing with positive control circ-HIPK3 to prove the amplification of circular RNA. According to the sequencing results, backsplicing junction of circ-HIPK3 was amplified via our experimental setup. Further, we started to validate differential expression of our candidates via qPCR. According to the initial results, candidate-8 was downregulated under apoptotic conditions in accordance with RNA-seq data. However, candidate-6 indicates upregulation under apoptotic conditions incompatible with RNA-seq data (Figure 3.12).

CHAPTER 5

CONCLUSION

In this study, identification and validation of circular RNAs differentially expressed in apoptotic HeLa cells were detected via deep sequencing, backsplicing junction validation and quantitative PCR.

After succesful drug screening experiments, HeLa cells were treated with four different agents to trigger apoptosis. After detection of differentially expressed circular RNAs, they were sorted based on their log change, drug-specificity and parental genes to choose circular RNA candidates. After that, their miRNA binding sites were identified in order to exhibit possible sponging mechanisms and literature search was done to investigate the involvement of these miRNAs in apoptosis. To that extend, hsa_let_7 and hsa_miR_106, which are involved in apoptosis, were identified commonly. Their possibility for translation were analysed bioinformatically. Candidate-6 and candidate-4 exhibited possibility for translation.

Circularity of candidates were checked by using RNAseR treated template. Thus, backsplicing junction (BSJ) of circ-HIPK3, candidate-8, candidate-5 and candidate-6 were shown. Circ-HIPK3 was used as positive control. Additionally, BSJ of circ-HIPK3 was sequenced by BIOMER IYTE. Based on qPCR results, candidate-8 and circ-HIPK3 indicated downregulation in apoptotic conditions but candidate-6 showed upregulation.

In conclusion, a comprehensive and systematic approach led to identification of differentially expressed 108, 234, 4 and 5 circRNAs upon treatments with CP, TNF-alpha, FAS and DOX, respectively (padj<0,05). Interestingly, TNF-alpha and CP caused diverse differential expression, however, DOX and FAS seems to be in accord with DMSO control group. Candidates might have phenotypic effect on apoptosis and might inhibit target gene expressions that are modulated by hsa_let_7, hsa_miR_106, hsa_miR_103 in apoptosis by sponging. As future direction, circular RNA candidates should be characterized functionally by overexpression and knockdown approach. Polysome profiling should be used to check the translation potential of candidate-6 and -4.

REFERENCES

Barrett S.P., Salzman J., Circular RNAs: analysis, expression and potential functions, Development, 143 (2016), 1838-1847.

Belle J., Petrov J.C., Langlais D., Robert F., Cencic R., Shen S., Pelletier J., Gros P., Nijnik A., Repression of p53-target gene Bbc3/PUMA by MYSM1 is essential for the survival of hematopoietic multipotent progenitors and contributes to stem cell maintenance, Cell Death Differ., 23 (2016), 759-775.

Bialik S., Zalckvar E., Ber Y., Rubinstein A.D., Kimchi A., Systems biology analysis of programmed cell death, Trends Biochem. Sci., 35 (2010), 556–564.

Bright J., Khar A., Apoptosis: programmed cell death in health and disease, Bipsci Rep., 14 (1994), 67-81.

Burd C.E., Jeck W.R., Liu Y., Sanoff H.K., Wang Z., Sharpless N.E., Expression of linear and novel circular forms of an INK4/ARF-associated non-coding RNA correlates with atherosclerosis risk, PLoS Genet., 6 (2010), 1-13.

Chinnaiyan A.M., The apoptosome: heart and soul of the cell death machine, Neoplasia, 1 (1999), 5–15.

Capel B., Swain A., Circular transcripts of the testis-determining gene Sry in adult mouse testis, Cell, 73 (1993), 1019–1030.

Chen L.L., The biogenesis and emerging roles of circular RNAs, Nat. Rev. Mol. Cell. Biol., 17 (2016), 205-211.

Chen L.L., Yang L., Regulation of circRNA biogenesis, RNA Biol., 12 (2015), 381-388.

Dang Y., Quyang X., Zhang F., Wang K., Lin Y., Sun B., Wang Y., Wang L., Huang Q., Circular RNAs expression profiles in human gastric cancer, Sci Rep., 7 (2017), 9060.

DeVries E.G.E., Gietema J.A., De Jong S., Tumor Necrosis Factor Related Apoptosis-Inducing Ligand Pathway and Its Therapeutic Implications, Clin Cancer Res., 12 (2006), 2390-3.

Dudekula D.B., Panda A.C., Grammatikakis I., De S., Abdelmohsen K., Gorospe M., CircInteractome: A web tool for exploring circular RNAs and their interacting proteins and microRNAs, 13 (2016), 34-42.

Edlich F., Banerjee S., Suzuki M., Cleland M.M., Arnoult D., Wang C., Neutzner A., Tjandra N., Youle RJ., Bcl-x(L) retrotranslocates Bax from the mitochondria into the cytosol, Cell, 145 (2011), 104-116.

Elmore S., Apoptosis: a review of programmed cell death, Toxicol Pathol., 35(2007), 495-516.

Enari M., Sakahira H., Yokoyama H., Okawa K., Iwamatsu A., Nagata S., A caspase-activated DNase that degrades DNA during apoptosis, and its inhibitor ICAD, Nature, 391 (1998), 43–50.

Fuchs Y., Programmed cell death in animal development and disease, Cell, 147 (2011), 742-758.

Tan M.L., Ooi J. P., Ismail N., Moad A.I., Muhammad T.S., Programmed cell death pathways and current antitumor targets, Pharmacol. Res., 26 (2009), 1547–1560.

Gaffo E., Bonizzato A., Kronnie G.T., Bortoluzzi S., CirComPara: A Multi-Method Comparative Bioinformatics Pipeline to Detect and Study circRNAs from RNA-seq Data, Non-conding RNA, 10 (2017), 8.

Gao.Y., Wang.J., CIRI: an efficient and unbiased algorithm for de novo circular RNA identification, Genome Biology, 16 (2015), 4.

Gao. Y., Zhang. J., Circular RNA identification based on multiple seed matching. Briefings in Bioinformatics, 19 (2017), 1–8.

Greene J., Baird A.M., Brady L., Lim M., Gray G.G., Raymond M., Finn S.P., Circular RNAs: Biogenesis, Function and Role in Human Diseases, 6 (2017), 4-38.

Griffith T.S., Brunner T., Fletcher S.M., Green D.R., Ferguson T.A., Fas ligand-induced apoptosis as a mechanism of immune privilege, Science, 17 (1995), 1189-92.

Hansen T. and Veno M., Comparison of circular RNA prediction tools, Nucleic Acids Research, 44 (2016), 58.

Hill M.M., Adrain C., Duriez P.J., Creagh E.M., Martin S.J., Analysis of the composition, assembly kinetics and activity of native Apaf-1 apoptosomes, Embo J., 23 (2004), 2134–45.

Holdt L.M., Stahringer A., Sass K., Pichler G., Kulak N.A., Wilfert W., Kohlmaier A., Herbst A., Northoff B.H., Nicolaou A., Gäbel G., Beutner F., Scholz M., Thiery J., Musunuru K., Krohn K., Mann M., Teupser D., Circular non-coding RNA ANRIL modulates ribosomal RNA maturation and atherosclerosis in humans, Nat Commun., 19 (2016), 12429.

Hsu H., Xiong J., Goeddel D.V., The TNF receptor 1-associated protein TRADD signals cell death and NF-kappa B activation, Cell, 81 (1995), 495–504.

Hsu M., Coca-Prados M., Electron microscopic evidence for the circular form of RNA in the cytoplasm and eukaryotic cell, Nature, 280 (1979), 339-340.

Huang G., Li S., Yang N., Zou Y., Zheng D., Xiao T., Recent progress in circular RNAs in human cancers, Cancer letters, 404 (2017), 8-18.

Igney F.H., Krammer P.H., Death and anti-death: tumour resistance to apoptosis, Nat. Rev. Cancer, 2 (2002), 277–288.

Jeck W.R., Sharpless N.E., Detecting and characterizing circular RNAs, Nat. Biotechnol., 32 (2014), 453-461.

Jin Z., El-Deiry W.S., Overwiev of cell death signalling pathways, Cancer Biol. Ther., 4 (2005), 139-163.

Jin Z., Wafik S., El-Deiry Z., Overview of cell death signaling pathways, Cancer Biology and Therapy, 4 (2005), 147-171.

Kaymaz B.T., Selvi N., Gokbulut A.A., Aktan C., Gündüz C., Saydam G., Sahin F., Cetintaş V.B., Baran Y., Kosova B., Suppression of STAT5A and STAT5B chronic myeloid leukemia cells via siRNA and antisense-oligonucleotide applications with the induction of apoptosis, Am J Blood Res, 3 (2013), 58-70.

Kelliher M.A., Grimm S., Ishida Y., Kuo F., Stanger B.Z., Leder P., The death domain kinase RIP mediates the TNF-induced NF-kappaB signal, Immunity, 8 (1998), 297–303.

Kerr J.F.R., Wyllie A.H., Currie A.R., Apoptosis: a basic biological phenomenon with wide-ranging implications in tissue kinetics, Br. J. Cancer, 26 (1972), 239–257.

Kos.A., Dijkema. R., The hepatitis delta (delta) virus possesses a circular RNA, Nature, 323 (1986), 558-560.

Kothakota S., Azuma T., Reinhard C., Klippel A., Tang J., Chu K., McGarry T.J., Kirschner M.W., Koths K., Kwiatkowski D.J., Williams L.T., Caspase-3-generated fragment of gelsolin: effector of morphological change in apoptosis, Science, 278 (1997), 294-298.

Kögel D., Prehn J.H.M., Caspase-Independent cell death mechanisms, Madame Curie Bioscience database, 2013.

Krishna S., Low I.C., Pervaiz S., Regulation of mitochondrial metabolism: yet another facet in the biology of the oncoprotein Bcl-2, Biochem J.,435 (2011), 545-551.

Kurosaka K., Takahashi M., Watanabe N., Kobayashi Y., Silent cleanup of very early apoptotic cells by macrophages, J. Immunol., 171 (2003), 4672–9.

Li L.Y., Luo X., Wang X., Endonuclease G is an apoptotic DNase when released from mitochondria, Nature 412 (2001), 95–9.

Martinvalet D., Zhu P., Lieberman J., GranzymeA induces caspase independent mitochondrial damage, a required first step for apoptosis, Immunity, 22 (2005), 355–70.

Mehta S.L., Pandi G., Vemuganti R., Circular RNA Expression Profiles Alter Significantly in Mouse Brain After Transient Focal Ischemia, A.h.a. journals, 48 (2017), 2451-2548.

Memczak S., Jens M., Elefsinioti A., Torti F., Krueger J., Rybak A., Maier L., Mackowiak S.D., Gregersen L.H., Munschauer M., Loewer A., Ziebold U., Landthaler M., Kocks C., Noble F., Rajewsky N., Circular RNAs are a large class of animal RNAs with regulatory potency, Nature, 495 (2013), 333-338.

Mokrejs M., Vopálenský V., Kolenaty O., Masek T., Feketová Z., Sekyrová P., Skaloudová B., Kríz V., Pospísek M., IRESite: the database of experimentally verified IRES structures, Nucleic acid research, 34 (2006), 125-30

Nan A., Chen L., Zhang N., Liu Z., Yang T., Wang Z., Yang C., Jiang Y., A novel regulatory network among LncRpa, CircRar1, MiR-671 and apoptotic genes promotes lead-induced neuronal cell apoptosis. Arch Toxicol, 91 (2016), 1671–1684.

Nigro J., Cho.K., Scrambled exons, Cell Press, 64 (1991), 607-613.

Pamudurti N.R., Bartok O., Jens M., Ashwal-Fluss R., Stottmeister C., Ruhe L., Hanan M., Wyler E., Perez-Hernandez D., Ramberger E., Shenzis S., Samson M., Dittmar G., Landthaler M., Chekulaeva M., Rajewsky N., Kadener S., Translation of CircRNAs, Mol. Cell, 66 (2017), 9-21.

Panda A.C., Detection and Analysis of Circular RNAs by RT-PCR, Bio. Protoc., 8 (2018), e2275.

Pena-Blanco A., Garcia-Saez A.J., Bax, Bak and beyond – mitochondrial performance in apoptosis, The FEBS Journal, 285 (2017), 416-431.

Pasman Z., Been M., Exon circularization in mammalian nuclear extracts, RNA, 2 (1996), 603-610.

Qu S., Yang X., Li X., Wang J., Gao Y., Shang R., Sun W., Dou K., Li H., Circular RNA: A new star of noncoding RNAs, Cancer Lett, 365 (2015), 141-148.

Ricci M.S., Kim S.H., Ogi K., Plastaras J.P., Ling J., Wang W., Jin Z., Liu Y.Y., Dicker D.T., Chiao P.J., Flaherty K.T., Smith C.D., El-Deiry W.S., Reduction of TRAIL-induced Mcl-1 and cIAP2 by c-Myc or sorafenib sensitizes resistant human cancer cells to TRAIL-induced death, Cancer cell, 12 (2007), 66-80.

Saelens X., Festjens N., Vande Walle L., Van Gurp M., Van Loo G., Vandenabeele P., Toxic proteins released from mitochondria in cell death, Oncogene, 23 (2004), 2861–74.

Sanger H., Klotz G., Viroids are single-stranded covalently closed circular RNA molecules existing as highly base-paired rod-like structures, Proceedings of the National Academy of Sciences of the United States of America, 73 (1976), 3852-3856.

Slee E.A., Adrain C., Martin S.J., Executioner caspase-3, -6, and -7 perform distinct, non-redundant roles during the demolition phase of apoptosis, J. Biol. Chem, 276 (2001), 7320–6.

Susin, S.A., Daugas E., Ravagnan L., Samejima K., Zamzami N., Loeffler M., Costantini P., Ferri K.F., Irinopoulou T., Prevost M.C., Brothers G., Mak T.W., Penninger J., Earnshaw W.C., Kroemer G., Two distinct pathways leading to nuclear apoptosis, J. Exp Med., 192(2000), 571–80.

Szabo L., Salzman J., Detecting circular RNAs: bioinformatic and experimental challenges, Nat Rev Genet., 17 (2016), 679-692.

Tait S.W., Green D., Mitochondria and cell death: outher membrane permeabilization and beyond, Nat. Rev. Mol. Cell Biol., 11 (2010), 621-32.

Taylor R.C., Cullen S.P., Martin S.J., Apoptosis: controlled demolition at the molecular level, Nat. Rev. Mol. Cell Biol., 9 (2008), 231-41.

Wajant H., The Fas signaling pathway: more than a paradigm, Science, 296 (2002), 1635–6.

Wang K, Gan T.Y., Li N., Liu C.Y., Zhou L.Y., Gao J.N., Circular RNA mediates cardiomyocyte death via miRNA-dependent upregulation of MTP18 expression, Cell Death Differ., 24 (2017), 1111-20.

Wang M., Yu F., Wu W., Zhang Y., Chang W., Ponnusamy M., Wang K., Li P., Circular RNAs: A novel type of non-coding RNA and their potential implications in antiviral immunity, Int. J. Biol. Sci., 13 (2017), 1497-1506.

Zhang L., Salzman J., Detecting circular RNAs: bioinformatic and experimental challenges, Nat. Rev. Genet., 17 (2016), 679-692.

Zhang Y., Xue W., Li X., Zhang J., Chen S., Zhang J.L., Yang L., Chen L.L. The Biogenesis of Nascent Circular RNAs, Cell Rep., 15 (2016), 611-624.

Zhang Y., Zhang X.O., Chen T., Xiang J.F., Yin Q.F., Xing Y.H. Zhu S., Yang L., Chen L.L., Circular intronic long noncoding RNAs, Mol. Cell, 51 (2013), 792-806.

Zheng Q., Bao C., Guo W., Li S., Chen J., Chen B., Luo Y., Lyu D., Li Y., Shi G., Liang L., Gu J., He X., Huang S., Circular RNA profiling reveals an abundant circHIPK3 that regulates cell growth by sponging multiple miRNAs, Nature Communications, 7 (2016), 1-13.

Yang Y., Fan X., Mao M., Song X., Wu P., Zhang Y., Jin Y., Yang Y., Chen L.L., Wang Y., Wong C.C., Xiao X., Wang Z., Extensive translation of circular RNAs driven by N6-methyladenosine, Cell. Res., 27 (2007), 626-641.